



An-Najah National University
Faculty of Graduate Studies

**FINITE VOLUME METHOD FOR
SOLVING NAVIER-STOKES
EQUATIONS IN FLUID DYNAMICS**

By
Abdulraheem Hussein Abu Arrah

Supervisor
Dr. Yahya Jaafra

**This Thesis is Submitted in Partial Fulfillment of the Requirements for the Degree
of Master of Computerized Mathematics, Faculty of Graduate Studies, An-Najah
National University, Nablus, Palestine.**

2025

FINITE VOLUME METHOD FOR SOLVING NAVIER-STOKES EQUATIONS IN FLUID DYNAMICS

By
Abdulraheem Hussein Abu Arrah

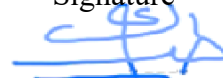
This Thesis was Defended Successfully on 24/06/2025 and approved by

Dr. Yahya Jaafra
Supervisor



Signature

Dr. Haneen Ghanem
External Examiner



Signature

Dr. Mohammad Yaseen
Internal Examiner



Signature

Dedication

This thesis is dedicated to my loving family, whose unwavering support and encouragement have been the driving force behind my academic journey. I am deeply grateful to my dear friends, who have provided laughter, camaraderie, and moments of respite amidst the academic rigors. And to all my relatives and loved ones who have stood by me with love and encouragement, this work is a testament to your belief in me.

Acknowledgments

Foremost, my grateful thanks to Allah, the almighty, for granting me the blessings and giving me the power and energy to conduct this humble work.

I would like to express my deepest gratitude to the discussion committee members, starting with my supervisor, Dr. Yahya Jaafra, for his guidance and encouragement, and the internal and external examiners, Dr. Mohammad Yaseen and Dr. Haneen Ghanem, for their time and generosity in reading this humble work.

I want to express my heartfelt gratitude to all those who have imparted knowledge to me, from the dedicated teachers of my school days to the esteemed professors and doctors at my university, An-Najah National University. Your dedication has had a huge impact on me.

Last but not least, I am grateful to everyone who has supported me in completing this dissertation.

Declaration

I, the undersigned, declare that I submitted the thesis entitled:

FINITE VOLUME METHOD FOR SOLVING NAVIER-STOKES EQUATIONS IN FLUID DYNAMICS

I declare that the work provided in this thesis, unless otherwise referenced, is the researcher's own work, and has not been submitted elsewhere for any other degree or qualification.

Student's Name: Abdul-Raheem Hussein Abu Arah

Signature: 

Date: 24/6/2025

List of Contents

Dedication	iii
Acknowledgments	iv
Declaration.....	v
List of Contents	vi
List of Tables	vii
List of Figures.....	viii
List of Appendices	ix
Abstract.....	x
Chapter One: Introduction	1
1.1 Fluid dynamics.....	1
1.2 Navier-Stokes Equations.....	2
Chapter Two: Governing Equations.....	5
2.1 Continuity Equation.....	5
2.2 Momentum Equation	8
2.3 Energy equation	12
2.4 General Governing Equation	14
2.5 Special Cases of Fluid dynamics	15
Chapter Three: Numerical Solutions.....	20
3.1 Finite Volume Method (FVM)	21
3.2 Finite Volume Schemes.....	32
3.2.1 Central differencing scheme	35
3.2.2 Upwind scheme.....	43
3.3 Schemes Comparison.....	48
Chapter Four: Navier-Stokes Equations By FVM	51
4.1 steady-state of Navier-Stokes equation in 1 dimension.....	51
4.2 Conclusion	58
List of Abbreviations	60
References.....	61
Appendices.....	64
الملخص	ب

List of Tables

Table 3.1: 2 iterations of ϕ distribution	30
Table 3.2: 10 iterations of ϕ distribution	30

List of Figures

Figure 2.1: Control volume for Eulerian technique	5
Figure 3.1: ϕ distribution along rod	22
Figure 3.2: Division rod into 5 control Volumes.....	26
Figure 3.3: Interior control volumes	26
Figure 3.4: West Boundary control volume	27
Figure 3.5: East Boundary control volume	28
Figure 3.6: Iterations and final distribution along the rod	31
Figure 3.7: Exact Solution Vs FVM solution of Diffusion equation	32
Figure 3.8: Central Difference Scheme with Gauss-Siedel (Pe = 3) and Upwind Scheme with Gauss-Siedel (Pe = 3)	49
Figure 4.1: Numerical Solution u(x) using fsolve.....	58

List of Appendices

Appendix A: MATLAB code for ϕ distribution along the rod by the finite volume method example.....	64
Appendix B: MATLAB code for Solving central difference scheme example	66
Appendix C: MATLAB code for Solving Upwind scheme example.....	69
Appendix D: MATLAB code for Solving Navier-Stokes example	72
Appendix E: Figures	74
Figure E.1: Neighbors of P control volume.....	74
Figure E.2: Division pipe into 5 control Volumes	74
Figure E.3: Interior control volumes	74
Figure E.4: West Boundary control volume	75
Figure E.5: East Boundary control volume	75
Figure E.6: Central Difference Scheme with Gauss-Siedel (Pe = 1.2).....	75
Figure E.7: Central Difference Scheme with Gauss-Siedel (Pe = 2).....	76
Figure E.8: Central Difference Scheme with Gauss-Siedel (Pe = 2.4).....	76
Figure E.9: Central Difference Scheme with Gauss-Siedel (Pe = 3).....	76
Figure E.10: Interior control volumes	77
Figure E.11: West Boundary control volume	77
Figure E.12: East Boundary control volume	77
Figure E.13: Upwind Scheme with Gauss-Siedel (Pe = 3)	77
Figure E.14: Upwind Scheme with Gauss-Siedel (Pe = 2)	78
Figure E.15: Upwind Scheme with Gauss-Siedel (Pe = 5)	78
Figure E.16: Upwind Scheme with Gauss-Siedel (Pe = 1.5)	78
Figure E.17: Division pipe into 5 control Volumes	78

FINITE VOLUME METHOD FOR SOLVING NAVIER-STOKES EQUATIONS IN FLUID DYNAMICS

By
Abdulraheem Hussein Abu Arrah
Supervisor
Dr. Yahya Jaafra

Abstract

Several equations, particularly the Navier-Stokes equations, govern fluid dynamics. These equations are essential for describing fluid motion, which helps us understand many natural phenomena. The Navier-Stokes equations present significant challenges for researchers in mathematics and engineering due to their complexity and the difficulties in obtaining analytical solutions. As a result, it has become necessary to explore alternative methods for solving these equations, particularly through numerical approaches. Since numerical methods yield approximate solutions, it is vital to evaluate the effectiveness of this approach in addressing the Navier-Stokes equations.

One such numerical method is the finite volume method (FVM), which provides approximate solutions to the Navier-Stokes equations. In this thesis, we conducted a thorough examination of the finite volume method using various examples of the Navier-Stokes equations that have analytical solutions. We began with simpler cases and gradually increased the complexity while also comparing our numerical results with the analytical solutions to assess how closely they aligned with the exact solutions. This comparison enabled us to evaluate the effectiveness of the method.

We encountered issues related to the stability and accuracy of the numerical solutions based on the specific conditions we examined while employing this method. As a result, we discussed the numerical schemes related to the Finite Volume Method (FVM) and the criteria for selecting a specific scheme, especially concerning the Peclet number. We then evaluated the effectiveness of each scheme by applying them to the same case.

The results obtained from the finite volume method for solving one-dimensional steady-state Navier-Stokes equations, with a suitable choice of discretization scheme, provided accurate solutions with excellent stability. However, we observed that when high Peclet numbers were used, solution instability emerged, necessitating the implementation of higher-order discretization schemes.

Future research could build on this method by looking at flow situations in two or three dimensions and improving computing efficiency with adaptive mesh refinement (AMR) and better discretization schemes.

Keywords: Finite Volume, Navier-Stokes Equations, Fluid Dynamics, Central Difference Scheme, Upwind Scheme, Peclet Number, Incompressible Flow, Convection-Diffusion, Numerical Solution, Continuity Equation, Momentum Equation, Energy Equation, Governing Equations.

Chapter One

Introduction

1.1 Fluid dynamics

Studying the kinetic behavior of fluids is the concentration of the physics and engineering field of fluid dynamics [1]. It encompasses a wide range of phenomena, such as simulating an aircraft wing to measure the flow of air over it or analyzing the movement of water in a river.

Fluid dynamics is the science that forms the basis for understanding and predicting how fluids interact with their surroundings, and this is very versatile and has many uses in both the business and non-business worlds. Among them are [1]:

1. Aviation and vehicle aerodynamics: lift and drag.
2. The dynamics of ships in water.
3. In a power plant, combustion occurs in gas turbines and internal combustion engines.
4. Equipment cooling, including microcircuits, is a subfield in electrical and electronic engineering.
5. Turbines and related machinery involve the study of fluid dynamics in revolving channels, diffusers, and other components.
6. Polymer molding and chemical process engineering include mixing and separation.
7. The building's interior and outside environments, including wind loads and HVAC.
8. Wastewater and pollution dispersion engineering focuses on the management of contaminants in marine environments.
9. River, estuary, and ocean flows; this is part of hydrology and oceanography.
10. Predictions in meteorology: weather.
11. Biomedical engineering illustrates the circulatory system, which includes the arteries and veins.

Computational fluid dynamics (CFD) is the computer-based modeling and analysis of systems including fluid flow, heat transport, and related phenomena like chemical reactions; it is a notion that emerges from all these applications.

Aircraft and jet engine design, R&D, and production have all benefited from computational fluid dynamics (CFD) methods from the 1960s and beyond [1]. Modern

internal combustion engines, gas turbine combustion chambers, and furnaces have all made use of these techniques.

Aircraft and jet engine design, R&D, and production have all benefited from computational fluid dynamics (CFD) methods from the 1960s and beyond [1]. Modern internal combustion engines, gas turbine combustion chambers, and furnaces have all made use of these techniques.

As for talking about fluid dynamics in general and the equations governing it and its properties, there are many books that dealt with this big and broad title, such as in [2,3,4,5,6].

1.2 Navier-Stokes Equations

The principles of conservation of mass, energy, and momentum form the basis of the Navier-Stokes equations, which are essential for comprehending fluid dynamics; this thesis will go into these three equations in more depth later on. These equations describe fluid behavior at various pressures and circumstances. The significance of studying these equations stems from the fact that they are used in various domains, including scientific inquiry, engineering applications, environmental knowledge, and technological innovation. There are several other causes [7].

Here are some points that illustrate the importance of these equations:

- Navier-Stokes equations accurately describe the motion and interaction of fluids with their surroundings, including the effects of viscosity and external forces.
- Navier-Stokes equations help engineers in aerospace field to designing efficient aircraft and spacecraft by understanding the mechanism of airflow over the wings and fuselage of the aircraft [8].
- Navier-Stokes equations assist civil engineers in designing structures such as bridges, dams, and buildings that can endure fluid stresses, as well as managing water flow in urban drainage systems [9].
- Assist cardiovascular researchers by analyzing blood flow in arteries and veins to understand cardiovascular diseases and develop medical devices such as stents and artificial heart valves [10].

There are many examples that cannot be counted in industrial applications, environmental and earth sciences, medical sciences, energy sciences and environmental engineering, even in terms of mathematical interest [11].

There are many studies that have dealt with this topic over time, and many researchers have studied it; for example, Sylvio Reynaldo Bistafa talks in [12] about the genesis of the Navier-Stokes equations and the revolution they made in understanding fluid motion by incorporating viscosity and friction into the equations. Matt Charnley in 2014 talked in his paper [13] about the derivation of the Navier-Stokes equations from physical principles, and Owe Axelsson discussed in [14] techniques for the numerical simulations of changing density incompressible fluids represented by the Navier-Stokes equations. It is especially essential for understanding numerical ways to solve these equations over time. Understanding these numerical methods is important when predicting fluid behavior in various applications, from engineering to meteorology. As researchers continue to explore advanced computational techniques, the potential for more accurate simulations of complex fluid dynamics becomes increasingly attainable.

To solve differential equations, one may use one of many popular numerical approaches, such as the finite difference method (FDM), the finite element method (FEM), or the finite volume method (FVM). Comparing the methods aims to determine their accuracy and efficiency and the possibility of using them in various fields. For numerical solutions to governing equations, many researchers talked about these methods. Mojumder, Md Shahadat Hossain talked in [15] about FDM for numerical analysis of one-dimensional heat equations, and LeVeque, Randall J., in his book [16], talked deeply about FDM as a numerical analytic method for generating approximate solutions to a broad range of engineering problems. FEM was discussed by Jagota, Vishal, and Sethi, and Aman Preet Singh in [17].

Regarding the method in which I intend to go deeper into this thesis, which is the method of FVM, Cardiff Philip and Demirdžić Ismet give in their study [18] an overview, background information, contrasting methods, and an evaluation of their merits; this is all done while keeping in close proximity to the gold standard in computational solid mechanics. An influential group of numerical techniques for estimating the solutions of hyperbolic partial differential equations was discussed in a book by Randall LeVeque, a professor of applied mathematics at the University of Washington and a Boeing Professor

[19]. Maliska, Clovis R., in his modern book [20], talked about FVM, about conservation equations, and about advection and diffusion interpolation functions. You can refer to these references to know more about numerical methods and their application [21, 22, 23].

Many scholars have tackled numerical solutions in their investigations, and Burmasheva, Natal'ya Vladimirovna, described the precise solution to the Navier-Stokes equation in [24]; the equation describes stratified fluid flows.

Using the work of Alexandre Joel Chorin in [25], a technique based on finite differences that may be used to solve the Navier-Stokes equations for an incompressible fluid that are time-dependent, in the article [26], Neaman Sohrabi and Dr. Karrar A. Hammoodi discussed the use of the finite volume approach to tackle the issue of heat transfer by observing the effects of various geometries on the quantity of heat transmission. Jian Li and Zhangxin Chen cover in [11] theoretical foundations, numerical schemes, and practical implementations of finite volume methods applied to incompressible Navier–Stokes equations.

Chapter Two

Governing Equations

To study the motion of liquids and gases (fluid dynamics), there is a set of equations that these fluids rely on that describe how these fluids behave under different conditions. These equations are called governing equations, where these equations are derived from the basic principles of the laws of conservation of energy, mass, and momentum.

The basic equations governing fluid dynamics are represented in these equations:

1. Continuity equation.
2. Momentum equations (Navier-Stokes equations).
3. Energy equation.

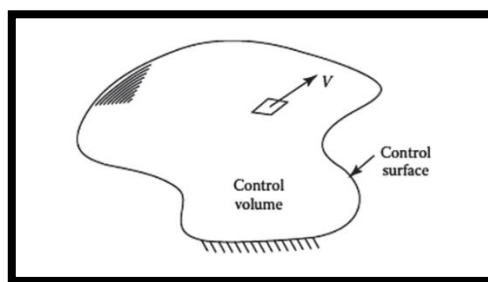
2.1 Continuity Equation

The following equation of continuity is obtained by applying the rule of conservation of mass to a fluid that is moving through an infinitesimal control volume that is stationary (see Figure 2.1) [27]:

$$\frac{\partial \rho}{\partial t} + \nabla \cdot (\rho \bar{U}) = 0 \dots\dots\dots (1)$$

Figure 2.1

Control volume for Eulerian technique



where ρ is the fluid density, \bar{U} is the fluid velocity.

The rate of density growth in the control volume is represented by the first term $\frac{\partial \rho}{\partial t}$ in this equation, while the rate of mass flux going out of the control surface (which surrounds the control volume) per unit volume is represented by the second term $\nabla \cdot (\rho \bar{U})$.

Equation (1) was obtained using the Eulerian method [27], which involves utilizing a fixed control volume and recording the changes to the fluid as it passes through the volume. Another Lagrangian method [27] involves tracking the evolution of a fluid element's characteristics while an observer moves in tandem with it. Fluid mechanics often uses the Eulerian perspective.

Equation (1) becomes [27] for a Cartesian coordinate system, where u , v , and w represent the x , y , and z components of the velocity vector:

$$\frac{\partial \rho}{\partial t} + \frac{\partial}{\partial x}(\rho u) + \frac{\partial}{\partial y}(\rho v) + \frac{\partial}{\partial z}(\rho w) = 0 \dots\dots\dots (2)$$

Note that:

$$\nabla = \frac{\partial}{\partial x} \bar{i} + \frac{\partial}{\partial y} \bar{j} + \frac{\partial}{\partial z} \bar{k}$$

and,

$$\bar{U} = u\bar{i} + v\bar{j} + w\bar{k}$$

now, multiply \bar{U} by ρ we get :

$$\rho\bar{U} = \rho u\bar{i} + \rho v\bar{j} + \rho w\bar{k}$$

now, multiplying ∇ by $\rho\bar{U}$, we get:

$$\nabla \cdot \rho\bar{U} = \frac{\partial \rho u}{\partial x} + \frac{\partial \rho v}{\partial y} + \frac{\partial \rho w}{\partial z}$$

The form of equation (2) is that of a conservation-law (divergence) equation.

In physics, the divergence form represents conservation laws, which state that a certain quantity within a system change only because it flows across the boundaries of the system (rather than being created or destroyed), this is often seen in fluid dynamics, electromagnetism, and heat transfer.

When the density of every component of the fluid stays the same, we say that the flow is incompressible. Mathematically, this implies that:

$$\frac{d\rho}{dt} = 0 \dots\dots\dots (3)$$

which leads to:

$$\nabla \cdot \bar{U} = 0 \dots\dots\dots (4)$$

or

$$\frac{\partial u}{\partial x} + \frac{\partial v}{\partial y} + \frac{\partial w}{\partial z} = 0 \dots\dots\dots(5)$$

for the Cartesian coordinate system.

The assumption of incompressibility is a suitable approximation, for instance, to get a constant flow of air with a velocity of less than 100 m/s or a mass of less than 0.3 [24].

The physical meaning, when you add the net entrance and exit to the partial change in mass, you get the entire change in mass, and here are equal to zero, in symbols:

$$\frac{D\rho}{Dt} = \frac{\partial\rho}{\partial t} + \nabla \cdot (\rho \bar{U}) = 0 \dots\dots\dots (6)$$

where $\frac{D}{Dt}$ is the material derivative, which stands for the rate at which a property changes

in a fluid that is in motion, $\frac{\partial\rho}{\partial t}$ is the local (Eulerian) derivative, which accounts for how

the property changes at a fixed point in space. This formula (equation 6) can be generalized to include more than one property, that is:

$$\frac{D(\rho\phi)}{Dt} = \frac{\partial(\rho\phi)}{\partial t} + \nabla \cdot (\rho \bar{U}\phi) \dots\dots\dots(7)$$

where ϕ any property, this form is called the conservative form.

2.2 Momentum Equation

Fluids are also regulated by the momentum equation, which states that the total force applied is equal to the change in momentum and is mostly derived from Newton's second law [20], that is:

$$\sum \bar{F} = \frac{d(m\bar{U})}{dt} \dots\dots\dots(8)$$

and we know that: $\rho = \frac{m}{v}$,

so: $m = \rho v$,

where \bar{F} : forces acting, m : mass, ρ : density, v : volume, that means:

$$\sum \bar{F} = \frac{d(\rho v \bar{U})}{dt},$$

and since the volume is constant so:

$$\frac{\sum \bar{F}}{v} = \frac{d(\rho \bar{U})}{dt}, \dots\dots\dots (9)$$

and this equation (9) has three directions, in x, y and z direction:

$$\frac{\sum F_x}{v} = \frac{d(\rho u)}{dt}, \frac{\sum F_y}{v} = \frac{d(\rho v)}{dt}, \text{ and } \frac{\sum F_z}{v} = \frac{d(\rho w)}{dt}, \dots\dots\dots (10)$$

but what forces act on fluids? The forces acting on fluids consist of three types: pressure force, shear force, and body force (such as gravity or weight), in symbols:

$-\nabla P$ represent the pressure force, $\nabla \cdot \tau$ represent the shear (viscous) force, and ρg represent the body force (gravity).

Now we can transform the formulas in (10) using the conservative form as mentioned earlier in (7) to:

$$\frac{\sum \mathbf{F}_x}{v} = \frac{d(\rho u)}{dt} = \frac{\partial(\rho u)}{\partial t} + \nabla \cdot (\rho u \bar{U}), \dots (11)$$

$$\frac{\sum \mathbf{F}_y}{v} = \frac{d(\rho v)}{dt} = \frac{\partial(\rho v)}{\partial t} + \nabla \cdot (\rho v \bar{U}), \dots (12)$$

$$\frac{\sum \mathbf{F}_z}{v} = \frac{d(\rho w)}{dt} = \frac{\partial(\rho w)}{\partial t} + \nabla \cdot (\rho w \bar{U}), \dots (13)$$

these equations (11), (12), and (13) can be expanded to include forces acting on fluids as mentioned above to get the x-momentum equation as follow:

$$\frac{\sum \mathbf{F}_x}{v} = \frac{d(\rho u)}{dt} = \frac{\partial(\rho u)}{\partial t} + \nabla \cdot (\rho u \bar{U}) = -\frac{\partial P}{\partial x} + \frac{\partial \tau_{xx}}{\partial x} + \frac{\partial \tau_{yx}}{\partial y} + \frac{\partial \tau_{zx}}{\partial z} + \rho \mathbf{g}_x, \dots (14)$$

when the normal tension operating on a surface perpendicular to the x-axis is denoted by τ_{xx} in the x-direction, these forces operate as compressive or tensile forces.

τ_{xy} : Deformation of a surface with respect to the x-axis due to shear stress occurring in the y-direction. This represents the internal force that causes deformation in the y-direction due to fluid flow along the x-axis.

τ_{xz} : Surface subjected to shear stress in the z-direction that is perpendicular to the x-axis. This represents deformation in the z-direction due to fluid flow along the x-axis [28].

Note that: $W = mg$

$$\text{then: } \frac{W}{v} = \frac{mg}{v} = \rho g.$$

The y-momentum equation is given by:

$$\frac{\sum \mathbf{F}_y}{v} = \frac{d(\rho v)}{dt} = \frac{\partial(\rho v)}{\partial t} + \nabla \cdot (\rho v \bar{U}) = -\frac{\partial P}{\partial y} + \frac{\partial \tau_{yx}}{\partial x} + \frac{\partial \tau_{yy}}{\partial y} + \frac{\partial \tau_{yz}}{\partial z} + \rho \mathbf{g}_y, \dots (15)$$

where: τ_{yx} : The x-direction shear stress operating on a surface that is perpendicular to the y-axis. This represents deformation in the x-direction due to fluid flow along the y-axis.

τ_{yy} : Constant y-directional tension applying on a y-axis-perpendicular surface. This represents compressive or tensile forces acting in the y-direction.

τ_{yz} : The z-direction shear stress operating on a surface that is perpendicular to the y-axis. This represents deformation in the z-direction due to fluid flow along the y-axis [28].

The z-momentum equation given as follow:

$$\frac{\sum \mathbf{F}_z}{v} = \frac{d(\rho w)}{dt} = \frac{\partial(\rho w)}{\partial t} + \nabla \cdot (\rho w \bar{\mathbf{U}}) = -\frac{\partial P}{\partial z} + \frac{\partial \tau_{zx}}{\partial x} + \frac{\partial \tau_{zy}}{\partial y} + \frac{\partial \tau_{zz}}{\partial z} + \rho \mathbf{g}_z \dots (16)$$

where: τ_{zx} : The x-direction shear stress acting on a z-perpendicular surface. This represents deformation in the x-direction due to fluid flow along the z-axis.

τ_{zy} : An y-direction shear stress operating on a z-perpendicular surface. This represents deformation in the y-direction due to fluid flow along the z-axis.

τ_{zz} : An ordinary z-normal stress operating on a z-perpendicular surface. This represents compressive or tensile forces acting in the z-direction [28].

The terms τ_{KL} , K=x,y,z and L=x,y,z are not related to partial derivatives. Instead, they are symbols representing stress tensor components. Other sections of the Navier-Stokes equations make use of partial derivatives (like the convective terms or viscous stress terms).

In a 3D fluid flow, the stress tensor τ is a matrix that looks like this[29]:

$$\tau = \begin{bmatrix} \tau_{xx} & \tau_{xy} & \tau_{xz} \\ \tau_{yx} & \tau_{yy} & \tau_{yz} \\ \tau_{zx} & \tau_{zy} & \tau_{zz} \end{bmatrix}.$$

Each component of this tensor tells you how much stress is being applied in a specific direction on a surface normal to one of the coordinate axes, where τ_{ij} is the shear stress

tensor, and Newton expressed by: $\tau_{ij} = \mu \frac{\partial u_i}{\partial x_j}$, where μ represents the dynamic viscosity

of the fluid. The internal resistance to flow of a fluid may be measured by its dynamic viscosity,

this leads to a custom kind of fluids called the Newtonian fluids.

So, for Newtonian fluids the momentums equations can be formed into[1]:

$$\text{x-momentum: } \frac{\partial(\rho u)}{\partial t} + \nabla \cdot (\rho u \bar{U}) = -\frac{\partial P}{\partial x} + \nabla \cdot (\mu \nabla u) + S_{Mx} + \rho g_x, \dots\dots\dots (17)$$

$$\text{y-momentum: } \frac{\partial(\rho v)}{\partial t} + \nabla \cdot (\rho v \bar{U}) = -\frac{\partial P}{\partial y} + \nabla \cdot (\mu \nabla v) + S_{My} + \rho g_y, \dots\dots\dots (18)$$

$$\text{z-momentum: } \frac{\partial(\rho w)}{\partial t} + \nabla \cdot (\rho w \bar{U}) = -\frac{\partial P}{\partial z} + \nabla \cdot (\mu \nabla w) + S_{Mz} + \rho g_z, \dots\dots\dots (19)$$

where in equation (17), $\frac{\partial(\rho u)}{\partial t}$ is called the unsteady term, $\nabla \cdot (\rho u \bar{U})$ is the convection term, $-\frac{\partial P}{\partial x}$ is the pressure force term (in x-direction per unit volume), $\nabla \cdot (\mu \nabla u)$ is viscous diffusion term, S_{Mx} is viscous source term or external sources of momentum (in x-direction), $\nabla \cdot (\mu \nabla u) + S_{Mx}$ is the shear stress term(in x-direction), and ρg_x called body force term (in x-direction per unit volume). Similarly for y-momentum and z-momentum equations.

The general momentum equation is expressed as [28]:

$$\frac{\partial(\rho u)}{\partial t} + \nabla \cdot (\rho \bar{U} u) = -\nabla p + \nabla \cdot \tau + \rho g, \dots\dots\dots(20)$$

where the term $\frac{\partial(\rho u)}{\partial t}$ represent the unsteady rate of change of momentum with respect to time, the term $\nabla \cdot (\rho \bar{U} u)$ represents the convective transport of momentum, the term $-\nabla p$ represents the force exerted by pressure gradients within the fluid, the term $\nabla \cdot \tau$ represents the divergence of the stress tensor which includes viscous forces, and the term ρg represents the body forces such as gravity acting on the fluid.

Since we will focus in our thesis on talking about Navier Stokes equation as a special case of momentum equations, it is a specific type of fluid, which is Newtonian fluids with an incompressible flow. As a result, in the case of a Newtonian fluid, the relationship between stress and strain rate is linear, the stress tensor τ can be decomposed into:

$$\tau = -p\mathbf{I} + \tau_{\text{viscous}}, \dots\dots\dots (21)$$

in where τ_{viscous} stands for the viscous stress tensor and \mathbf{I} is the identity matrix.

The formula for the viscous stress tensor of a Newtonian fluid is:

$$\tau_{\text{viscous}} = \mu(\nabla\mathbf{u} + (\nabla\mathbf{u})^T) - \frac{2}{3}\mu(\nabla\cdot\mathbf{u})\mathbf{I}, \dots\dots\dots (22)$$

here, μ is the dynamic viscosity, and $(\nabla\mathbf{u})^T$ is the transpose of the velocity gradient tensor.

The equation is simplified to the Navier-Stokes equation for an incompressible flow by substituting (22) into (20), (where $\nabla\cdot\mathbf{u} = 0$):

$$\rho\left(\frac{\partial\mathbf{u}}{\partial t} + (\mathbf{u}\cdot\nabla)\mathbf{u}\right) = -\nabla p + \mu\nabla^2\mathbf{u} + \rho\mathbf{g}, \dots\dots\dots (23)$$

where $\frac{\partial\mathbf{u}}{\partial t}$ is the unsteady or time-dependent acceleration, $(\mathbf{u}\cdot\nabla)\mathbf{u}$ is the convective acceleration which representing how the velocity field influences itself through space, $-\nabla p$ is pressure gradient force that driving the fluid flow, $\mu\nabla^2\mathbf{u}$ is the viscous diffusion term representing internal friction due to viscosity, and $\rho\mathbf{g}$ express the external forces like gravity.

2.3 Energy equation

The following energy equation follows the stages of applying the first law of thermodynamics to a fluid moving through an infinitesimal, fixed control volume:

To start, keep in mind what the first law of thermodynamics states:

$$\dot{Q} - \dot{W} = \frac{dE}{dt} \dots\dots\dots (24)$$

also, we mentioned earlier that in equation (7):

$$\frac{d(\rho\phi)}{dt} = \frac{\partial(\rho\phi)}{\partial t} + \nabla \cdot (\rho \bar{U}\phi) . (7)$$

Now, remember that:

$$E = U + KE + PE ,$$

above, E stands for total energy, U for internal energy, KE for kinetic energy, and PE for potential energy; but, in this situation, we only have internal energy to represent total energy, and both kinetic and potential energy are zero, so,

$$E = U ,$$

and since,

$$U = mc_v T ,$$

where m is the mass, c_v is the specific heat capacity at constant volume, and T is the temperature, so we get:

$$E = mc_v T ,$$

so when substitute E in equation (24) we get:

$$\dot{Q} - \dot{W} = \frac{d(mc_v T)}{dt} ,$$

and when divide the equation on the volume v we get:

$$\frac{\dot{Q}}{v} - \frac{\dot{W}}{v} = \frac{d(\rho c_v T)}{dt} ,$$

and when use the formula by equation (7) we get [1]:

$$\frac{\partial(\rho c_v T)}{\partial t} + \nabla \cdot (\rho c_v T \bar{U}) = -P(\nabla \cdot \bar{U}) + \nabla \cdot (K \nabla T) + S + \Phi \dots\dots\dots (25)$$

where the variable $\frac{\partial(\rho c_v T)}{\partial t}$ stands for the rate of change of internal energy per unit volume over time, the term $\nabla \cdot (\rho c_v T \bar{U})$ represents the convective transport of internal energy, $-P(\nabla \cdot \bar{U})$ is the work done by pressure term, $\nabla \cdot (K \nabla T)$ is the diffusion term with K thermal conductivity and ∇T is temperature gradient, S is the volumetric heat source term, and the word that describes the process by which viscous forces cause the transformation of kinetic energy into internal energy is denoted as Φ .

Equation (25) is the third equation that fluids depend on; it is known as the energy equation.

2.4 General Governing Equation

The continuity, momentum, and energy equations—all of which regulate fluids—have been discussed in isolation, we can express all these equations in the following general form [30]:

$$\frac{\partial(\rho \phi)}{\partial t} + \nabla \cdot (\rho \phi \bar{U}) = \nabla \cdot (\Gamma \nabla \phi) + S, \dots\dots\dots (26)$$

where:

1. as a function of time, $\frac{\partial(\rho \phi)}{\partial t}$ shows how much the carried amount ϕ per unit volume is changing, where ρ is the quantity being conveyed (such as velocity, temperature, etc.) and ϕ is the fluid's density.
2. $\nabla \cdot (\rho \phi \bar{U})$ is the convection term that represent the convective transport of the quantity ϕ where \bar{U} is the velocity vector of the fluid.
3. $\nabla \cdot (\Gamma \nabla \phi)$ is the diffusion term that represent the diffusive transport of the quantity ϕ where Γ is the diffusion coefficient (can be mass diffusivity, momentum diffusivity,

or thermal conductivity depending on the context), and $\nabla\phi$ is the gradient of the transported quantity ϕ , and S Represents any sources or sinks of the quantity ϕ .

Using this general equation we can obtain all governing equations that we talked about earlier by changing the variable ϕ and the diffusion coefficient Γ , so to get the continuity equation for example, we substitute the variable $\phi=1$. To get the momentum equations we change the variable ϕ by the component of velocity and Γ by the dynamic viscosity, and when $\phi=T$ (temperature) and Γ is the thermal conductivity the equation will represent the energy equation.

Note that the diffusion term $\nabla\cdot(\Gamma\nabla\phi)$ can be analyzed in its directional components as follows:

$$\nabla\cdot(\Gamma\nabla\phi) = \frac{\partial}{\partial x}(\Gamma \frac{\partial\phi}{\partial x}) + \frac{\partial}{\partial y}(\Gamma \frac{\partial\phi}{\partial y}) + \frac{\partial}{\partial z}(\Gamma \frac{\partial\phi}{\partial z}),$$

and if Γ is constant we get:

$$\Gamma\nabla\cdot(\nabla\phi) = \Gamma\nabla^2\phi,$$

then:

$$\Gamma\nabla\cdot(\nabla\phi) = \Gamma(\frac{\partial^2\phi}{\partial x^2} + \frac{\partial^2\phi}{\partial y^2} + \frac{\partial^2\phi}{\partial z^2}).$$

The equation: $\Gamma\nabla\cdot(\nabla\phi) = \Gamma\nabla^2\phi$,

describes the diffusive transport of a scalar quantity ϕ in a medium. The operator $\nabla^2\phi$ called the Laplacian operator that quantifies how ϕ spreads out in space due to diffusion, and Γ is the diffusion coefficient that determines the rate of this diffusion.

2.5 Special Cases of Fluid dynamics

Fluid dynamics can be addressed in many special cases based on several classifications that can be considered. The first classification that we will deal with depends on the types of flow, and then we will deal with another classification based on flow trends. There

may be special cases that depend on the combination of the two classifications; we will talk about some of them after talking about each classification separately.

First of all, with regard to the first classification based on flow types [31], we can categorize fluid dynamics by different types of flows into:

1. Steady flow: at every given location in the flow field, the fluid characteristics remain constant throughout this flow type.
2. Unsteady flow: Fluid characteristics undergo temporal changes in this flow type, which may occur anywhere in the flow field.
3. Compressible flow: In this particular flow pattern, the fluid's density fluctuates substantially over the flow field.
4. Incompressible flow [32]: Within this particular flow type, the fluid's density stays rather constant.
5. Laminar flow: this type of flow is characterized by smoothness and arrangement of motion by layers of fluid sliding past each other.
6. Turbulent flow: this type is characterized by irregular chaotic movement with swirls and swirls of fluids.
7. Boundary layer flow: In this type of flow, the viscous effects are significant when the flow is near a solid boundary.

Many types we only mention them without the need to address the details of their definitions, like potential flow, rotational flow, irrotational flow, internal flow, and external flow, etc.

Each of the above cases presents a different set of challenges, and to solve fluid flow problems effectively requires different analytical or numerical approaches.

You may explain the fluid's motion using a combination of more than one of the preceding situations, and combining these cases helps to give an accurate description of the flow under study.

Examples where multiple cases are used together:

1. Steady and Incompressible Flow
2. Steady, Incompressible, and Laminar Flow
3. Steady, Incompressible, and Turbulent Flow

4. Unsteady and Compressible Flow
5. Steady, Rotational, and Incompressible Flow
6. Unsteady, Compressible, and Turbulent Flow

and many cases can be addressed or imposed.

This combination often simplifies the governing equations that these fluids are governed by, making these equations solvable and making it easier to solve complex flow problems.

The second consideration by which fluids can be classified is flow direction; this consideration may increase complexity and detail in fluid dynamics analysis. This classification includes how a fluid moves with respect to a particular frame of reference or special object. Examples of major directional flow situations include [31]:

1. Flow with Just One Spatial Dimension (1D): Here, flow characteristics change along a single spatial axis.
2. Two-Dimensional (2D) Flow: In this case, flow properties vary in two spatial dimensions, with negligible variation in the third dimension.
3. Three-Dimensional (3D) Flow: In this case, the properties of the flow differ in all three directions.
4. Radial Flow: Here flow in fluid moves radially inward or outward from a central point.
5. Parallel Flow: In this type of flow, streamlines are parallel to each other, often approximating unidirectional flow.

and other cases, such as perpendicular (cross) flow and axial flow.

As mentioned earlier, we can combine the two classifications in certain special cases where they combine directional cases with other flow conditions, and examples of that are

1. Steady, Incompressible, and 2D Flow
2. Unsteady, Compressible, and 3D Flow
3. Radial and Laminar Flow
4. Axial and Turbulent Flow

This combination of flow direction cases and other flow conditions makes describing and analyzing fluids more comprehensive, and this makes it easier to understand the behavior of fluids.

To illustrate how the previous special cases help simplify the governing equations that have been mentioned, we will give the following example:

Example1: For incompressible two-dimension fluid, write and simplify the continuity equation and the energy equation.

Solution:

1. remember the continuity equation is:

$$\frac{\partial \rho}{\partial t} + \nabla \cdot (\rho \bar{U}) = 0$$

since the fluid is incompressible; that is meaning ρ is constant so,

$$\frac{\partial \rho}{\partial t} = 0,$$

and the term $\nabla \cdot (\rho \bar{U})$ become $\rho \nabla \cdot \bar{U}$ then we get:

$$\nabla \cdot \bar{U} = 0,$$

and since the fluid in two dimensions; the equation:

$$\nabla \cdot \bar{U} = 0,$$

will become:

$$\frac{\partial u}{\partial x} + \frac{\partial v}{\partial y} = 0,$$

and this equation, which is a simplified version of the continuity equation.

2. remember the energy equation is:

$$\frac{\partial \rho c_v T}{\partial t} + \nabla \cdot (\rho c_v T \bar{U}) = -P(\nabla \cdot \bar{U}) + \nabla \cdot (K \nabla T) + S + \Phi,$$

since the fluid is incompressible and in two-dimensions the term:

$$\frac{\partial \rho c_v T}{\partial t} + \nabla \cdot (\rho c_v T \bar{U}),$$

will become:

$$\rho \left(\frac{\partial c_v T}{\partial t} + \left(\frac{\partial c_v T u}{\partial x} + \frac{\partial c_v T v}{\partial y} \right) \right).$$

The term $-P(\nabla \cdot \bar{U})$ will be zero from the continuity equation ($\nabla \cdot \bar{U} = 0$), the term $\nabla \cdot (K \nabla T)$ will become:

$$\frac{\partial}{\partial x} \left(k \frac{\partial T}{\partial x} \right) + \frac{\partial}{\partial y} \left(k \frac{\partial T}{\partial y} \right),$$

then the equation of energy in a simple form is:

$$\rho \left(\frac{\partial c_v T}{\partial t} + \left(\frac{\partial c_v T u}{\partial x} + \frac{\partial c_v T v}{\partial y} \right) \right) = \frac{\partial}{\partial x} \left(k \frac{\partial T}{\partial x} \right) + \frac{\partial}{\partial y} \left(k \frac{\partial T}{\partial y} \right) + S + \Phi.$$

Chapter Three

Numerical Solutions

The Navier-Stokes equations and other governing equations may be solved in several ways, from analytical solutions to numerical solutions, of course, according to the data and hypotheses for each problem separately.

As for analytical solutions, they are used in some simple cases, or these equations can be made simpler—I mean the Navier-Stokes equations—through assumptions that facilitate access to the analytical solution. A student can easily find a formula for the flow speed u based on the radius r by solving the simpler one-dimensional momentum equation for steady laminar flow in a pipe. Similarly, by solving heat transfer problems, students learn to determine the rate at which a pipe's heat transfer rate decreases as a function of the thickness of the insulation. In both instances, the equations are one-dimensional and, although they originated as partial differential equations (PDEs), they are now classified as ordinary differential equations (ODEs).

Analytical solutions are seldom feasible for the Navier-Stokes equations due to their complexity and nonlinearity; therefore, numerical solutions are necessary to obtain results.

These solutions may deal with complex geometry, nonlinear equations, and multiscale events, giving extensive insights into fluid behavior. They may also simulate time-dependent flow problems, such as turbulent flows, and perform parameter analysis and optimization. Numerical solutions also allow for the visualization and analysis of flow variables, as well as the precise calculation of quantities such as drag, lift, and heat transfer. They also offer cost-effective alternatives to physical experiments, making them ideal for industries such as aerospace and automotive engineering. Numerical simulations can help develop novel theories and models in fluid dynamics, such as turbulence modeling and flow instability. They check and validate theoretical models to ensure their accuracy.

Navier-Stokes equations may be solved numerically using various approaches, such as:

1. Finite Difference Method (FDM) [30]: This method uses simple calculations to estimate the changes in the Navier-Stokes equations by breaking the area into a grid

of points. These equations are then solved recursively by updating the values until convergence occurs.

2. Finite Volume Method (FVM) [30]: By dividing the domain into control volumes, the Navier-Stokes equations may be integrated using the finite volume technique. This approach involves calculating unknowns across the centers of cells and mass, momentum, and energy fluxes across the faces of volumes. This method is especially famous when dealing with complex geometric shapes because it has conservation properties.
3. The third approach is the finite element technique (FEM), which means dividing the area into many smaller pieces and then changing the Navier-Stokes equations into a problem that looks for the best solution. This method is more suitable when dealing with irregular geometric shapes and gives more accurate results than FDM and FVM since it depends on reducing the potential energy in the fluid system based on the boundary conditions.
4. Additional approaches include the Lattice Boltzmann Method (LBM), Direct Numerical Simulation (DNS), Large Eddy Simulation (LES), and others.

All the above methods differ from each other in accuracy, complexity, applicability, and computational cost. The choice of one of these methods depends on the specific focus of the researcher, such as the desired level of accuracy. The decision also relies on the difficulty of the issue to be addressed, the circumstances surrounding it, and the complexity of the problem.

In my thesis, I will focus on the finite volume method, as I mentioned earlier, because of its properties in conserving energy, momentum, and mass and the possibility of dealing with complex geometric shapes, and because Navier-Stokes equations are somewhat complex and not easy to solve by analytical methods.

3.1 Finite Volume Method (FVM)

Particularly in domains like fluid dynamics, the finite volume approach finds extensive use in solving partial differential equations, heat transfer, and other fields that are based on conservation laws. The integral form of the governing equations is the mainstay of this approach, making it well-suited to issues pertaining to the conservation of mass, momentum, and energy.

To clarify this method and how it works at the outset, it is necessary to recall the general formula of the governing equations that we dealt with earlier, which is:

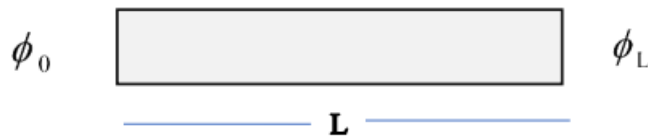
$$\frac{\partial(\rho\phi)}{\partial t} + \nabla \cdot (\rho\phi\bar{U}) = \nabla \cdot (\Gamma\nabla\phi) + S \dots\dots\dots(26)$$

And now we will apply this equation to an example to see what the finite volume method will be like. Through this example, we will review and explain the steps that the finite volume method goes through.

Example 2: Rod has a length L, with $\phi_0 = 100 \text{ }^\circ\text{C}$ and $\phi_L = 200 \text{ }^\circ\text{C}$, find the ϕ distribution (heat distribution) along the rod by the finite volume method. (see Figure 3.1)

Figure 3.1

ϕ distribution along rod



Steps:

The first step to solve equation (26), we need to simplify the equation because we can't deal with the equation with the current form, so we will assume the following:

1. Steady. ($\frac{\partial\rho\phi}{\partial t} = 0$)
2. Diffusion only. ($\nabla \cdot (\rho\phi\bar{U}) = 0$) (we can solve the equation with convection only or convection and diffusion).
3. One dimension(x-dimension).
4. Source free (no heat generation), ($S = 0$).

So, the equation (26) becomes:

$$\nabla \cdot (\Gamma\nabla\phi) = 0$$

and when we decompose it, we get:

$$\frac{\partial}{\partial x}(\Gamma \frac{\partial \phi}{\partial x}) + \frac{\partial}{\partial y}(\Gamma \frac{\partial \phi}{\partial y}) + \frac{\partial}{\partial z}(\Gamma \frac{\partial \phi}{\partial z}) = 0,$$

and since our assumption is in one dimension, the equation becomes:

$$\frac{d}{dx}(\Gamma \frac{d\phi}{dx}) = 0,$$

and now we want to solve it by the finite volume method.

Step two, discretization using the finite volume approach, follows the simplification of the equation.

The finite volume method divides the domain into control volumes. Each control volume has an east face and a west face. Then, there are two more control volumes surrounding each control volume. In the middle of each control volume, you'll find the names and data of the control volumes. When we divide the domain, we care about the control volume itself, not about their neighbors east and west. (See Figure E1 in Appendix E.)

Now, we integrate the equation:

$$\frac{d}{dx}(\Gamma \frac{d\phi}{dx}) = 0,$$

on the P control volume, we get:

$$\iiint \frac{d}{dx}(\Gamma \frac{d\phi}{dx}) dv = 0,$$

and since the cross-section area is fixed the triple integral has no meaning, so we get:

$$\int_w^e \frac{d}{dx}(\Gamma \frac{d\phi}{dx}) A dx = 0,$$

implies:

$$\Gamma A \frac{d\phi}{dx} \Big|_w^e = 0,$$

then:

$$\Gamma A \left| \frac{d\phi}{dx} \right|_e - \Gamma A \left| \frac{d\phi}{dx} \right|_w = 0,$$

and since $\Gamma A = \text{constant}$, we get:

$$\left. \frac{d\phi}{dx} \right|_e - \left. \frac{d\phi}{dx} \right|_w = 0$$

This is the first method, as a second method for discretizing the domain according to the divergence theorem [20]:

$$\iiint \nabla \cdot (\Gamma \nabla \phi) dv = \iint \hat{n} \cdot (\Gamma \nabla \phi) dA,$$

remember that:

$$\nabla = \frac{\partial}{\partial x} \bar{i} + \frac{\partial}{\partial y} \bar{j} + \frac{\partial}{\partial z} \bar{k},$$

multiply by ϕ gives:

$$\nabla \phi = \frac{\partial \phi}{\partial x} \bar{i} + \frac{\partial \phi}{\partial y} \bar{j} + \frac{\partial \phi}{\partial z} \bar{k},$$

so, when we return to our integral:

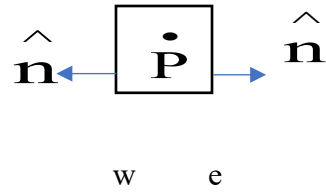
$$\iiint \nabla \cdot (\Gamma \nabla \phi) dv = 0,$$

then by divergence theorem:

$$\iiint \nabla \cdot (\Gamma \nabla \phi) dv = \iint \hat{n} \cdot (\Gamma \nabla \phi) dA = 0,$$

and since we deal in one dimension in x-direction we get:

$$\iint \hat{n} \cdot \left(\Gamma \frac{d\phi}{dx} \bar{i} \right) dA = 0,$$



then:

$$\Gamma A \left. \frac{d\phi}{dx} \right|_e - \Gamma A \left. \frac{d\phi}{dx} \right|_w = 0$$

and since ΓA is constant then:

$$\left. \frac{d\phi}{dx} \right|_e - \left. \frac{d\phi}{dx} \right|_w = 0,$$

This result is identical to the one obtained from the first method of discretization, which we will use in the subsequent steps; let's refer to it as equation (27).

This explains how to use the central difference to estimate the first derivative at the control volume's faces, which is needed to approximate the derivatives of this result or equation (27):

$$\left. \frac{d\phi}{dx} \right|_e = \left. \frac{d\phi}{dx} \right|_{x_{i+\frac{1}{2}}} \approx \frac{\phi_{i+1} - \phi_i}{\Delta x},$$

and $\left. \frac{d\phi}{dx} \right|_w = \left. \frac{d\phi}{dx} \right|_{x_{i-\frac{1}{2}}} \approx \frac{\phi_i - \phi_{i-1}}{\Delta x},$

use these estimates in place of the full equation:

$$\frac{\phi_{i+1} - \phi_i}{\Delta x} - \frac{\phi_i - \phi_{i-1}}{\Delta x} = 0,$$

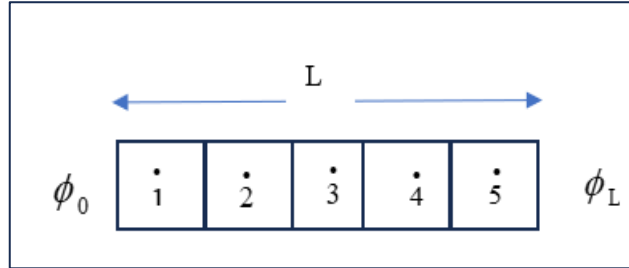
combine the terms implies:

$$\frac{\phi_{i+1} - 2\phi_i + \phi_{i-1}}{\Delta x^2} = 0,$$

Now that we have the discretization result, we will move on to Geometry and Mesh, where we divide the rod into five control volumes to make it easier to deal with in our example, as in (Figure 3.2).

Figure 3.2

Division rod into 5 control Volumes



The control volume number 1 is called the west boundary since it has an east neighbor only; the control volumes number 2, 3, and 4 are called the interior control volumes since they have an east neighbor and a west neighbor; and the control volume number 5 is called the east boundary since it has a west neighbor only.

Let $L = 1$ meter

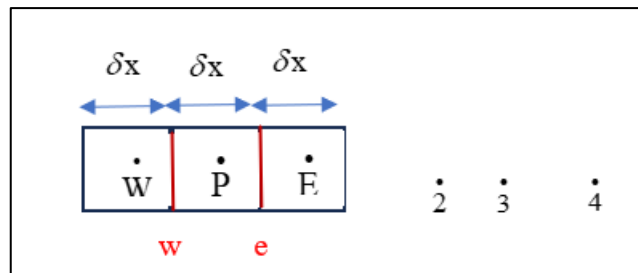
$$\delta x = \frac{L}{\text{no. of elements}} = \frac{1}{5}$$

$$\Rightarrow \delta x = 0.2$$

The fourth step in our solution is to take the result represented by equation (27) and apply it at the interior control volumes (2, 3, 4) (see Figure 3.3) as follows:

Figure 3.3

Interior control volumes



$$\left. \frac{d\phi}{dx} \right|_e - \left. \frac{d\phi}{dx} \right|_w = 0,$$

$$\frac{\phi_E - \phi_P}{\delta x} - \frac{\phi_P - \phi_W}{\delta x} = 0,$$

$$\phi_E - 2\phi_P + \phi_W = 0,$$

that implies:

$$\phi_W - 2\phi_P + \phi_E = 0,$$

so, for control volume 2, we get:

$$\phi_1 - 2\phi_2 + \phi_3 = 0 \dots (2),$$

and, for control volume 3, we get:

$$\phi_2 - 2\phi_3 + \phi_4 = 0 \dots (3),$$

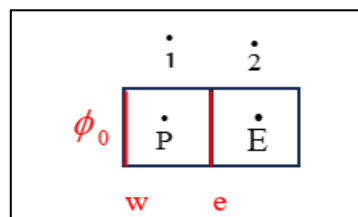
and, for control volume 4, we get:

$$\phi_3 - 2\phi_4 + \phi_5 = 0 \dots (4),$$

Now, we will move to apply equation (27) at control volume number 1, called (the west boundary) (see Figure 3.4):

Figure 3.4

West Boundary control volume



$$\left. \frac{d\phi}{dx} \right|_e - \left. \frac{d\phi}{dx} \right|_w = 0,$$

$$\frac{\phi_E - \phi_P}{\delta x} - \frac{\phi_P - \phi_0}{\delta x/2} = 0,$$

$$\phi_E - 3\phi_P + 2\phi_0 = 0,$$

then:

$$-3\phi_P + \phi_E = -2\phi_0,$$

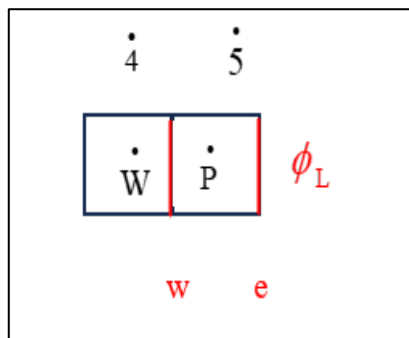
so, for control volume number 1, we get:

$$-3\phi_1 + \phi_2 = -2\phi_0 \dots (1),$$

and now, we will apply equation (27) at control volume number 5 called (the east boundary) (see Figure 3.5):

Figure 3.5

East Boundary control volume



$$\left. \frac{d\phi}{dx} \right|_e - \left. \frac{d\phi}{dx} \right|_w = 0,$$

$$\frac{\phi_L - \phi_P}{\delta x/2} - \frac{\phi_P - \phi_W}{\delta x} = 0,$$

$$2\phi_L - 3\phi_P + \phi_W = 0,$$

then:

$$\phi_W - 3\phi_P = -2\phi_L,$$

so, for control volume number 5, we get:

$$\phi_4 - 3\phi_5 = -2\phi_L \dots (5)$$

Now, we have five equations with five unknowns as follows:

$$\begin{aligned}
-3\phi_1 + \phi_2 &= -2\phi_0 \quad \dots (1) \\
\phi_1 - 2\phi_2 + \phi_3 &= 0 \quad \dots (2) \\
\phi_2 - 2\phi_3 + \phi_4 &= 0 \quad \dots (3) , \\
\phi_3 - 2\phi_4 + \phi_5 &= 0 \quad \dots (4) \\
\phi_4 - 3\phi_5 &= -2\phi_L \quad \dots (5)
\end{aligned}$$

and we can transform these equations to matrix form as follows:

$$\begin{bmatrix} -3 & 1 & 0 & 0 & 0 \\ 1 & -2 & 1 & 0 & 0 \\ 0 & 1 & -2 & 1 & 0 \\ 0 & 0 & 1 & -2 & 1 \\ 0 & 0 & 0 & 1 & -3 \end{bmatrix} \begin{bmatrix} \phi_1 \\ \phi_2 \\ \phi_3 \\ \phi_4 \\ \phi_5 \end{bmatrix} = \begin{bmatrix} -2\phi_0 \\ 0 \\ 0 \\ 0 \\ -2\phi_L \end{bmatrix} ,$$

the coefficient matrix represents a special type of matrices called Tri Diagonal Matrix that have many features which facilitate access to the solution.

Now, we want to solve this system using one of iteration methods as Jacobi method as follows:

$$\begin{aligned}
\phi_1 &= \frac{\phi_2 + 2\phi_0}{3} \quad \dots (1) \\
\phi_2 &= \frac{\phi_1 + \phi_3}{2} \quad \dots (2) \\
\phi_3 &= \frac{\phi_2 + \phi_4}{2} \quad \dots (3) , \\
\phi_4 &= \frac{\phi_1 + \phi_5}{2} \quad \dots (4) \\
\phi_5 &= \frac{\phi_4 + 2\phi_L}{3} \quad \dots (5)
\end{aligned}$$

the first iteration will be between the ϕ_0 and ϕ_L , assume it equal to 150 as follow in the table:

Table 3.1*2 iterations of ϕ distribution*

Iteration	ϕ_1	ϕ_2	ϕ_3	ϕ_4	ϕ_5
0	150	150	150	150	150
1	116.667	150	150	150	183.33
2	116.667	133.33	150	166.667	183.33

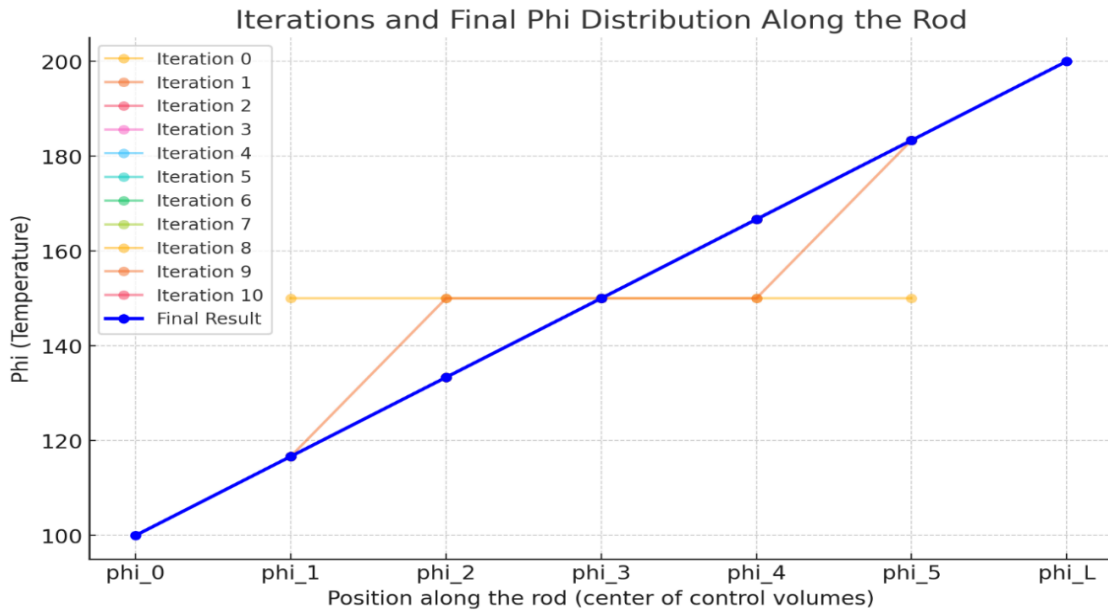
And we can continue to as many iterations as we want, say to 10 iterations, for example, as shown in the following table and figure:

Table 3.2*10 iterations of ϕ distribution*

Iteration	ϕ_1	ϕ_2	ϕ_3	ϕ_4	ϕ_5
0	150.000	150.000	150.000	150.000	150.000
1	116.667	150.000	150.000	150.000	183.330
2	116.667	133.330	150.000	166.667	183.330
3	116.665	133.334	149.999	166.665	183.334
4	116.667	133.332	149.999	166.666	183.333
5	116.666	133.333	149.999	166.666	183.333
6	116.667	133.332	149.999	166.666	183.333
7	116.666	133.333	149.999	166.666	183.333
8	116.666	133.333	149.999	166.666	183.333
9	116.666	133.333	149.999	166.666	183.333
10	116.667	133.333	149.999	166.666	183.333

Figure 3.6

Iterations and final distribution along the rod



Here is the graph showing the ϕ values over 10 iterations using the Jacobi method. Each line represents the distribution of ϕ along the rod at a specific iteration. As you can see, the solution converges quickly, with the interior values stabilizing after just a few iterations.

The final solution or the final distribution of ϕ 's along the rod is given by:

$$\phi_1 \approx 116.667^\circ\text{C}, \phi_2 \approx 133.333^\circ\text{C}, \phi_3 \approx 149.999^\circ\text{C}, \phi_4 \approx 166.666^\circ\text{C}, \phi_5 \approx 183.333^\circ\text{C},$$

As one would anticipate from a steady-state heat conduction issue with constant boundary conditions and no internal heat creation, the final distribution shows a nearly linear gradient in temperature down the rod.

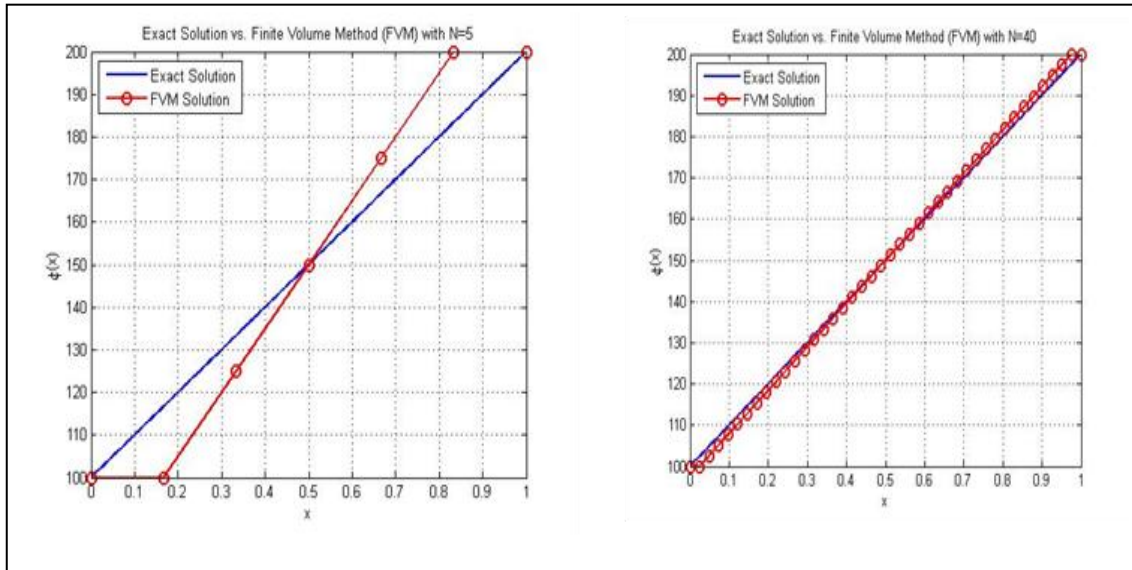
The following code demonstrates the finite volume method solution with the precise solution for the preceding steady-state diffusion equation. It eliminates the requirement for iteration techniques and allows us to directly solve the system using the MATLAB software (see Appendix A).

FVM Solution using MATLAB (see Figure 3.7):

110.0000, 130.0000, 150.0000, 170.0000, 190.0000

Figure 3.7

Exact Solution Vs FVM solution of Diffusion equation



3.2 Finite Volume Schemes

Since most practical issues cannot be solved analytically, we must rely on numerical solutions, such as the finite volume approach, to regulate fluid motion. These solutions are based on nonlinear partial differential equations, such as the Navier-Stokes equations.

To get approximations of solutions to governing equations, the domain is discretized using the finite volume approach. These solutions vary in accuracy and stability according to numerical schemes used to approximate main terms such as convection, diffusion, and pressure terms.

Numerical schemes approximate the fluxes of quantities like momentum, energy, and mass across the control volume faces that we got from dividing the domain using the finite volume method. These schemes will greatly influence the determination of the overall accuracy and stability of the solution.

Since the different physical processes' representation of the main terms of governing equations, such as convection and diffusion terms, we need to approximate them numerically. The convection term represents the transport of quantities like momentum or temperature due to the flow of the fluid, while the diffusion term represents the spread of these quantities due to molecular interactions. These terms, as mentioned earlier, are discretized at the faces of control volumes, and this discretization will be varied according

to numerical schemes that are used, and the choice of numerical schemes directly affects the accuracy and stability of the solution.

In the finite volume method, numerical schemes can be classified based on the treatment of diffusion and convection terms; also, these schemes vary in the accuracy order and stability condition. Schemes may have accuracy levels ranging from first-order to higher-order; they can also be stable or unstable, depending on the situation and the fact that they are time-dependent. At the same time, there can be schemes with high accuracy but at the expense of stability and complexity.

The choice of numerical schemes depends on more than one reason, and before diving into the details of these schemes, I will touch here to talk about one of the reasons that plays a key role in choosing the right scheme, which is the Peclet Number.

The Peclet number (Pe) is a quantity that characterizes the relative importance between convection and diffusion during the process of heat, momentum, and mass transport through the fluid. It is widely used in fluid dynamics to determine which physical process dominates in a given system. In other words, the Peclet number quantifies the ratio of a quantity's convective transport to its diffusive transit in a physical setting [33]. One way to describe the Peclet number is as:

$$Pe = \frac{LU}{\alpha} = \frac{LU}{D}, \dots\dots\dots (28)$$

where:

For example, the domain size or the length scale of interest may be represented by L, the characteristic length. The flow's typical velocity is denoted by U.

α is the thermal diffusivity (used in heat transfer problems).

D is the mass diffusivity (used in mass transfer problems).

Here the Peclet number can be one of three cases as follows:

1. $Pe \gg 1$: Convection-dominated flow: In this case, the effect of convection is much higher than diffusion. This happens, for example, in fast-flowing liquids.

2. $Pe \ll 1$: Diffusion-dominated flow: In this case the effect of diffusion is much higher than convection; this happens, for example, in slow-flowing liquids.
3. $Pe \approx 1$: Harmonized convection and diffusion: when the effects of both processes are comparable, a condition of balance is achieved.

These cases of the Peclet number play a main role in determining the numerical schemes that should be used in the finite volume method as follows:

1- Convection schemes, like upwind schemes, are used when the Peclet number is high, which is an indication that convection dominates over diffusion. It is preferred to use them because they ensure numerical stability. Using other schemes in this regime, like using central differencing, can lead to oscillations and instability.

2-Diffusion schemes: like central difference schemes, used when the Peclet number is low, it is an indication that diffusion dominates over convection. These schemes are more appropriate since they give better accuracy to describe the diffusive behavior. Using other schemes in this regime, like using upwind schemes, can lead to less accurate solutions.

It is essential to discuss realistic thresholds in the context of discussing convection and diffusion schemes, whether in the finite volume technique or numerical methods generally, the behavior of numerical schemes isn't only determined by whether Pe is much greater or much less than 1. Instead, practical considerations for stability and accuracy introduce specific thresholds like $Pe = 2$; at $Pe = 2$ there is two cases can be occurred:

1. Below $Pe = 2$: central difference scheme works very well because diffusion smoothes out the solution.
2. Above $Pe = 2$: central difference scheme leads to instability oscillations because convection becomes significant enough, that require another scheme like upwind differencing for stability.

This shows the correlation between physical classification and numerical behavior of schemes.

In order not to make a defect in the understanding of the above about Pe, let's summarize the above:

1. Physical classification: Pe classifies flows into diffusion dominated when $Pe \ll 1$ and convection dominated when $Pe \gg 1$.
2. Numerical Scheme Selection: the threshold $Pe = 2$ within convection dominated flows defines where the central difference becomes unstable and upwind difference is needed.

This is how we explain the physical interpretation of Pe for practical numerical considerations.

3.2.1 Central differencing scheme

The central differencing approach approximates derivatives or fluxes with second-order accuracy.

It computes the flow at a control volume face by averaging the values of adjacent cells, yielding a balanced and symmetric representation.

Considering the 1D steady-state convection-diffusion equation, as stated in Section 2.1, we get the governing equation as follows, which allows us to go into the derivation of this scheme. This builds on our previous work in explaining the general technique in the finite volume method (FVM):

$$\nabla \cdot (\rho \phi \bar{U}) = \nabla \cdot (\Gamma \nabla \phi) \dots\dots\dots (29)$$

This equation can be further simplified as a one-dimension into[20]:

$$\frac{d}{dx} (\rho \phi u) = \frac{d}{dx} \left(\Gamma \frac{d\phi}{dx} \right) \dots\dots\dots (30)$$

After the equation is simplified, the second step is to discretize it using the finite volume technique. In order to discretize the domain using the finite volume technique, it is separated into control volumes. The preceding image depicted this procedure (see Figure E1 in appendix E):

Now, we integrate governing equation (29) on the P control volume we get:

$$\iiint \nabla \cdot (\rho \phi \bar{U}) dv = \iiint \nabla \cdot (\Gamma \nabla \phi) dv, \dots\dots\dots (31)$$

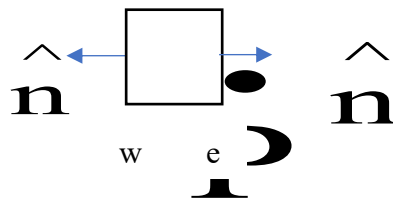
as well as the result of using the divergence theorem:

$$\begin{aligned} \iiint \nabla \cdot (\rho \phi \bar{U}) dv &= \oiint \hat{n} \cdot (\rho \phi \bar{U}) dA, \\ \iiint \nabla \cdot (\Gamma \nabla \phi) dv &= \oiint \hat{n} \cdot (\Gamma \nabla \phi) dA, \end{aligned}$$

so the equation (31) get:

$$\oiint \hat{n} \cdot (\rho \phi \bar{U}) dA = \oiint \hat{n} \cdot (\Gamma \nabla \phi) dA, \dots\dots\dots (32)$$

as seen in the following picture, with \hat{n} being the vector perpendicular to the area:



and since we deal in one dimension in x-direction we get:

$$\oiint \hat{n} \cdot (\rho \phi u \hat{i}) dA = \oiint \hat{n} \cdot (\Gamma \frac{d\phi}{dx} \hat{i}) dA,$$

then:

$$\rho \phi A u \Big|_e - \rho \phi A u \Big|_w = \Gamma A \frac{d\phi}{dx} \Big|_e - \Gamma A \frac{d\phi}{dx} \Big|_w,$$

assuming ρ , u , and A are constants we get:

$$\rho u (\phi_e - \phi_w) = \Gamma \left(\frac{d\phi}{dx} \Big|_e - \frac{d\phi}{dx} \Big|_w \right), \quad (33)$$

now, let's assume that we have a pipe with a fluid with u velocity into the pipe, and this fluid transfers heat by convection and diffusion, and we want to mesh for it as follows (see Figure E2 in Appendix E):

Assume $L=1$ meter.

$$\delta x = \frac{L}{\text{no. of elements}} = \frac{1}{5}$$

$$\Rightarrow \delta x = \frac{1}{5}$$

$$\text{Péclet Number} = \text{Pe} = \frac{\text{convection}}{\text{diffusion}} = \frac{\rho u \delta x}{\Gamma}$$

The next step in our solution, that is take the result represented by equation (33) and apply it at the interior control volumes (2,3,4) as follows (see Figure E3 in Appendix E):

$$\text{so: } \rho u (\phi_e - \phi_w) = \Gamma \left(\frac{d\phi}{dx} \Big|_e - \frac{d\phi}{dx} \Big|_w \right),$$

then by Taylor:

The gradient at the east face is approximated as [20]:

$$\frac{d\phi}{dx} \Big|_e = \frac{\phi_E - \phi_P}{\delta x} = \frac{\phi_{i+1} - \phi_i}{\delta x},$$

the gradient at the west face is approximated as [20]:

$$\frac{d\phi}{dx} \Big|_w = \frac{\phi_P - \phi_W}{\delta x} = \frac{\phi_i - \phi_{i-1}}{\delta x},$$

thus, the diffusive terms are:

$$\left[\Gamma \frac{d\phi}{dx} \right]_e = \Gamma \frac{\phi_{i+1} - \phi_i}{\delta x}, \quad \left[\Gamma \frac{d\phi}{dx} \right]_w = \Gamma \frac{\phi_i - \phi_{i-1}}{\delta x},$$

and regarding the convective flux:

Using central differencing, we can estimate the value of ϕ at the east face [20]:

$$\phi_e = \frac{\phi_E + \phi_P}{2} = \frac{\phi_{i+1} + \phi_i}{2},$$

and the value of ϕ at the west face is approximated using central differencing[20]:

$$\phi_w = \frac{\phi_P + \phi_W}{2} = \frac{\phi_i + \phi_{i-1}}{2},$$

thus, the convective flux terms are:

$$[\rho u \phi]_e = \rho u \frac{\phi_{i+1} + \phi_i}{2}, \quad [\rho u \phi]_w = \rho u \frac{\phi_i + \phi_{i-1}}{2},$$

now, if we substituting the diffusive and convective flux terms into the flux balance equation (equation 33) we get the following:

$$\rho u \left[\frac{\phi_{i+1} + \phi_i}{2} - \frac{\phi_i + \phi_{i-1}}{2} \right] = \Gamma \left[\frac{\phi_{i+1} - \phi_i}{\delta x} - \frac{\phi_i - \phi_{i-1}}{\delta x} \right],$$

simplify the terms we get:

$$\rho u \frac{1}{2} [\phi_{i+1} - \phi_{i-1}] = \frac{\Gamma}{\delta x} [\phi_{i+1} - 2\phi_i - \phi_{i-1}],$$

$$\frac{\delta x \rho u}{\Gamma} \frac{1}{2} [\phi_{i+1} - \phi_{i-1}] = [\phi_{i+1} - 2\phi_i - \phi_{i-1}],$$

$$\left(\frac{1}{2} \text{Pe}\right) [\phi_{i+1} - \phi_{i-1}] = [\phi_{i+1} - 2\phi_i - \phi_{i-1}],$$

where $\text{Pe} = \frac{\delta x \rho u}{\Gamma}$, so:

$$\left(\frac{-\text{Pe}}{2} - 1\right)\phi_{i-1} + 2\phi_i + \left(\frac{\text{Pe}}{2} - 1\right)\phi_{i+1} = 0,$$

this is the general form that we can used in the interior points (2,3, and 4) as follows to get 3 equations, at point 2:

$$\left(\frac{-Pe}{2} - 1\right)\phi_1 + 2\phi_2 + \left(\frac{Pe}{2} - 1\right)\phi_3 = 0,$$

at point 3:

$$\left(\frac{-Pe}{2} - 1\right)\phi_2 + 2\phi_3 + \left(\frac{Pe}{2} - 1\right)\phi_4 = 0,$$

and at point 4:

$$\left(\frac{-Pe}{2} - 1\right)\phi_3 + 2\phi_4 + \left(\frac{Pe}{2} - 1\right)\phi_5 = 0,$$

now, we will move to apply equation (33) at control volume number 1 called (the west boundary) (see Figure E4 in Appendix E):

$$\rho u(\phi_e - \phi_w) = \Gamma \left(\frac{d\phi}{dx} \Big|_e - \frac{d\phi}{dx} \Big|_w \right),$$

the value of ϕ at the east face is approximated using central differencing:

$$\phi_e = \frac{\phi_E + \phi_P}{2} = \frac{\phi_{i+1} + \phi_i}{2},$$

and the value of ϕ at the west face is:

$$\phi_w = \phi_0,$$

and regarding the gradient at the east face is approximated as:

$$\frac{d\phi}{dx} \Big|_e = \frac{\phi_E - \phi_P}{\delta x} = \frac{\phi_{i+1} - \phi_i}{\delta x},$$

and the gradient at the west face is approximated as:

$$\frac{d\phi}{dx} \Big|_w = \frac{\phi_P - \phi_0}{\delta x / 2},$$

now, substitute ϕ_w , ϕ_e , $\frac{d\phi}{dx} \Big|_w$, $\frac{d\phi}{dx} \Big|_e$ in equation (33) will get:

$$\rho u \left(\frac{\phi_E + \phi_P}{2} - \phi_0 \right) = \Gamma \left(\frac{\phi_E - \phi_P}{\delta x} - \frac{\phi_P - \phi_0}{\delta x / 2} \right),$$

$$\rho u \left(\frac{\phi_E + \phi_P}{2} - \phi_0 \right) = \frac{\Gamma}{\delta x} (\phi_E - 3\phi_P + 2\phi_0),$$

$$\frac{\delta x \rho u}{\Gamma} \left(\frac{\phi_E + \phi_P}{2} - \phi_0 \right) = (\phi_E - 3\phi_P + 2\phi_0),$$

$$\text{Pe} \left(\frac{\phi_E + \phi_P}{2} - \phi_0 \right) = (\phi_E - 3\phi_P + 2\phi_0) ,$$

where: $\text{Pe} = \frac{\delta x \rho u}{\Gamma}$, then:

$$\left(\frac{\text{Pe}}{2} + 3 \right) \phi_P + \left(\frac{\text{Pe}}{2} - 1 \right) \phi_E = (2 + \text{Pe}) \phi_0,$$

apply at point 1 get:

$$\left(\frac{\text{Pe}}{2} + 3 \right) \phi_1 + \left(\frac{\text{Pe}}{2} - 1 \right) \phi_2 = (2 + \text{Pe}) \phi_0,$$

and next, we will move to apply equation (33) at control volume number 5 called (the east boundary) (see Figure E5 in Appendix E):

$$\rho u (\phi_e - \phi_w) = \Gamma \left(\frac{d\phi}{dx} \Big|_e - \frac{d\phi}{dx} \Big|_w \right),$$

the value of ϕ at the east face is:

$$\phi_e = \phi_L$$

and the value of ϕ at the west face is approximated using central differencing:

$$\phi_w = \frac{\phi_P + \phi_W}{2} = \frac{\phi_1 + \phi_{1-1}}{2},$$

and regarding the gradient at the east face is approximated as:

$$\frac{d\phi}{dx} \Big|_e = \frac{\phi_L - \phi_P}{\delta x / 2},$$

and the gradient at the west face is approximated as:

$$\frac{d\phi}{dx} \Big|_w = \frac{\phi_P - \phi_W}{\delta x},$$

now, substitute ϕ_w , ϕ_e , $\frac{d\phi}{dx} \Big|_w$, $\frac{d\phi}{dx} \Big|_e$ in equation (33) will get:

$$\rho u \left(\phi_L - \frac{\phi_P + \phi_W}{2} \right) = \Gamma \left(\frac{\phi_L - \phi_P}{\delta x / 2} - \frac{\phi_P - \phi_W}{\delta x} \right),$$

$$\rho u \left(\phi_L - \frac{\phi_P + \phi_W}{2} \right) = \frac{\Gamma}{\delta x} (2\phi_L - 3\phi_P + \phi_W),$$

$$\frac{\delta x \rho u}{\Gamma} \left(\phi_L - \frac{\phi_P + \phi_W}{2} \right) = (2\phi_L - 3\phi_P + \phi_W),$$

$$\text{Pe} \left(\phi_L - \frac{\phi_P + \phi_W}{2} \right) = (2\phi_L - 3\phi_P + \phi_W) \quad ,$$

where: $\text{Pe} = \frac{\delta x \rho u}{\Gamma}$,

$$\left(\frac{-\text{Pe}}{2} - 1 \right) \phi_W + \left(\frac{-\text{Pe}}{2} + 3 \right) \phi_P = (2 - \text{Pe}) \phi_L,$$

apply at point 5:

$$\left(\frac{-\text{Pe}}{2} - 1 \right) \phi_4 + \left(\frac{-\text{Pe}}{2} + 3 \right) \phi_5 = (2 - \text{Pe}) \phi_L,$$

now, we have five equations with five unknowns as follows:

$$\left(\frac{\text{Pe}}{2} + 3 \right) \phi_1 + \left(\frac{\text{Pe}}{2} - 1 \right) \phi_2 = (2 + \text{Pe}) \phi_0 \quad \dots (1),$$

$$\left(\frac{-\text{Pe}}{2} - 1 \right) \phi_1 + 2\phi_2 + \left(\frac{\text{Pe}}{2} - 1 \right) \phi_3 = 0 \quad \dots (2),$$

$$\left(\frac{-Pe}{2}-1\right)\phi_2 + 2\phi_3 + \left(\frac{Pe}{2}-1\right)\phi_4 = 0 \quad \dots (3),$$

$$\left(\frac{-Pe}{2}-1\right)\phi_3 + 2\phi_4 + \left(\frac{Pe}{2}-1\right)\phi_5 = 0 \quad \dots (4),$$

$$\left(\frac{-Pe}{2}-1\right)\phi_4 + \left(\frac{-Pe}{2}+3\right)\phi_5 = (2-Pe)\phi_L \dots (5),$$

and we can transform these equations to matrix form as follows:

$$\begin{bmatrix} \left(\frac{Pe}{2}+3\right) & \left(\frac{Pe}{2}-1\right) & 0 & 0 & 0 \\ \left(\frac{-Pe}{2}-1\right) & 2 & \left(\frac{Pe}{2}-1\right) & 0 & 0 \\ 0 & \left(\frac{-Pe}{2}-1\right) & 2 & \left(\frac{Pe}{2}-1\right) & 0 \\ 0 & 0 & \left(\frac{-Pe}{2}-1\right) & 2 & \left(\frac{Pe}{2}-1\right) \\ 0 & 0 & 0 & \left(\frac{-Pe}{2}-1\right) & \left(\frac{-Pe}{2}+3\right) \end{bmatrix} \begin{bmatrix} \phi_1 \\ \phi_2 \\ \phi_3 \\ \phi_4 \\ \phi_5 \end{bmatrix} = \begin{bmatrix} (2+Pe)\phi_0 \\ 0 \\ 0 \\ 0 \\ (2-Pe)\phi_L \end{bmatrix},$$

the coefficient matrix called the tridiagonal matrix that has many features that facilitate access to the solution.

This system can be solved in more than one way, like Jacobi or Gauss-Seidel or the backward direct method. I'm going to solve this system using the Gauss-Seidel method because it has faster convergence than the Jacobi method using MATLAB coding (see Appendix B).

MATLAB results: (see Figures E6,E7,E8 and E9 in Appendix E)

The above results show the difference in the result depending on the Pe variation, it is very evident through the results instability in the results when the $Pe > 2$, this confirms what we have already mentioned in terms of stability around the use of this scheme and that there will be stable when $Pe \leq 2$ and instability and oscillations when $Pe > 2$.

As for accuracy, this scheme has second-order accuracy in space as follows:

The central differencing scheme approximates derivatives using Taylor series expansions:

$$\left. \frac{d\phi}{dx} \right|_p = \frac{\phi_E - \phi_W}{2\Delta x},$$

ignoring higher-order terms in the Taylor expansion results in the truncation error.

$$\phi_E = \phi_p + \Delta x \frac{\partial \phi}{\partial x} + \frac{\Delta x^2}{2} \frac{\partial^2 \phi}{\partial x^2} + O(\Delta x^3),$$

substituting back will get:

$$\text{Truncation Error} \propto O(\Delta x^2),$$

this demonstrates the second-order spatial accuracy of the central differencing scheme.

3.2.2 Upwind scheme

The upwind scheme is a numerical method for simulating the convection component of the convection-diffusion equation, which is useful in cases when convection is more important than diffusion. (i.e., for large Peclet numbers, $Pe > 2$).

Because the central difference scheme causes fluctuations and instability when $Pe > 2$, another scheme must be used in order to address this state of instability and oscillation, which is Upwind scheme.

To evaluate this scheme, we need to use the same conditions and example as the one we used for the 1D steady-state convection-diffusion equation in the previous scheme.

So that there is no kind of boredom from repeating the previous steps, I'll go straight to the step where we need to use rounding with the Upwind scheme, from equation (33):

$$\rho u (\phi_e - \phi_w) = \Gamma \left(\left. \frac{d\phi}{dx} \right|_e - \left. \frac{d\phi}{dx} \right|_w \right), \dots\dots\dots (33)$$

However, it is crucial to remember that this method considers the flow direction, and the answer changes depending on that direction ($u > 0$ or $u < 0$).

So, we can take the case of flow direction ($u > 0$) that happened when the flow was from left to right. Now, we apply equation (33) at the interior control volumes (2, 3, 4) as follows (see Figure E10 in Appendix E):

Using the Upwind technique, we can estimate the value of ϕ at the east face [10,20]:

$$\phi_e = \phi_p = \phi_i,$$

whereas the Upwind technique is used to estimate the value of ϕ at the west face [20]:

$$\phi_w = \phi_w = \phi_{i-1},$$

thus, the convective flux terms are:

$$[\rho u \phi]_e = \rho u \phi_i, \quad [\rho u \phi]_w = \rho u \phi_{i-1},$$

and regarding to the diffusive flux:

by Taylor: the gradient at the east face is approximated as:

$$\left. \frac{d\phi}{dx} \right|_e = \frac{\phi_E - \phi_P}{\delta x} = \frac{\phi_{i+1} - \phi_i}{\delta x},$$

the gradient at the west face is approximated as:

$$\left. \frac{d\phi}{dx} \right|_w = \frac{\phi_P - \phi_W}{\delta x} = \frac{\phi_i - \phi_{i-1}}{\delta x},$$

thus, the diffusive terms are:

$$\left[\Gamma \frac{d\phi}{dx} \right]_e = \Gamma \frac{\phi_{i+1} - \phi_i}{\delta x}, \quad \left[\Gamma \frac{d\phi}{dx} \right]_w = \Gamma \frac{\phi_i - \phi_{i-1}}{\delta x},$$

now, if we substituting the diffusive and convective flux terms into the flux balance equation (equation 33) we get the following:

$$\rho u (\phi_i - \phi_{i-1}) = \Gamma \left(\frac{\phi_{i+1} - \phi_i}{\delta x} - \frac{\phi_i - \phi_{i-1}}{\delta x} \right),$$

$$\rho u (\phi_i - \phi_{i-1}) = \frac{\Gamma}{\delta x} (\phi_{i+1} - 2\phi_i + \phi_{i-1}),$$

$$\frac{\rho u \delta x}{\Gamma} (\phi_i - \phi_{i-1}) = (\phi_{i+1} - 2\phi_i + \phi_{i-1}),$$

$$\text{Pe}(\phi_1 - \phi_{1-1}) = (\phi_{1+1} - 2\phi_1 + \phi_{1-1}) ,$$

where: $\text{Pe} = \frac{\rho u \delta x}{\Gamma}$,

rearrange the terms get:

$$(1 + \text{Pe})\phi_{1-1} + (-2 - \text{Pe})\phi_1 + \phi_{1+1} = 0,$$

this is the general form that we can use in the interior points (2,3, and 4) as follows to get 3 equations: at point 2:

$$(1 + \text{Pe})\phi_1 + (-2 - \text{Pe})\phi_2 + \phi_3 = 0,$$

at point 3:

$$(1 + \text{Pe})\phi_2 + (-2 - \text{Pe})\phi_3 + \phi_4 = 0,$$

at point 4:

$$(1 + \text{Pe})\phi_3 + (-2 - \text{Pe})\phi_4 + \phi_5 = 0,$$

now, we will move to apply equation (33) at control volume number 1 called (the west boundary), (see Figure E11 in Appendix E):

$$\rho u(\phi_e - \phi_w) = \Gamma \left(\frac{d\phi}{dx} \Big|_e - \frac{d\phi}{dx} \Big|_w \right),$$

the value of ϕ at the east face is approximated using Upwind scheme:

$$\phi_e = \phi_p = \phi_1,$$

the value of ϕ at the west face is approximated using Upwind scheme:

$$\phi_w = \phi_0,$$

regarding the gradient at the east face is approximated as:

$$\left. \frac{d\phi}{dx} \right|_e = \frac{\phi_E - \phi_P}{\delta x} = \frac{\phi_{i+1} - \phi_i}{\delta x},$$

and the gradient at the west face is approximated as:

$$\left. \frac{d\phi}{dx} \right|_w = \frac{\phi_P - \phi_0}{\delta x / 2},$$

now, substitute ϕ_w , ϕ_e , $\left. \frac{d\phi}{dx} \right|_w$, $\left. \frac{d\phi}{dx} \right|_e$ in equation (33) will get:

$$\rho u (\phi_P - \phi_0) = \Gamma \left(\frac{\phi_E - \phi_P}{\delta x} - \frac{\phi_P - \phi_0}{\delta x / 2} \right),$$

$$\rho u (\phi_P - \phi_0) = \frac{\Gamma}{\delta x} (\phi_E - 3\phi_P + 2\phi_0),$$

$$\frac{\delta x \rho u}{\Gamma} (\phi_P - \phi_0) = (\phi_E - 3\phi_P + 2\phi_0),$$

$$\text{Pe} (\phi_P - \phi_0) = (\phi_E - 3\phi_P + 2\phi_0) ,$$

$$\text{where: } \text{Pe} = \frac{\delta x \rho u}{\Gamma},$$

$$(-\text{Pe} - 3)\phi_P + \phi_E = (-\text{Pe} - 2)\phi_0,$$

apply at point 1 get:

$$(-\text{Pe} - 3)\phi_1 + \phi_2 = (-\text{Pe} - 2)\phi_0,$$

next, we will move to apply equation (33) at control volume number 5 called (the east boundary)(see Figure E12 in Appendix E):

$$\rho u (\phi_e - \phi_w) = \Gamma \left(\left. \frac{d\phi}{dx} \right|_e - \left. \frac{d\phi}{dx} \right|_w \right),$$

the value of ϕ at the east face is:

$$\phi_e = \phi_p = \phi_1,$$

and the value of ϕ at the west face is approximated using central differencing:

$$\phi_w = \phi_w = \phi_{i-1},$$

regarding the gradient at the east face is approximated as:

$$\left. \frac{d\phi}{dx} \right|_e = \frac{\phi_L - \phi_p}{\delta x / 2},$$

the gradient at the west face is approximated as:

$$\left. \frac{d\phi}{dx} \right|_w = \frac{\phi_p - \phi_w}{\delta x},$$

now, substitute ϕ_w , ϕ_e , $\left. \frac{d\phi}{dx} \right|_w$, $\left. \frac{d\phi}{dx} \right|_e$ in equation (33) will get:

$$\rho u (\phi_p - \phi_w) = \Gamma \left(\frac{\phi_L - \phi_p}{\delta x / 2} - \frac{\phi_p - \phi_w}{\delta x} \right),$$

$$\rho u (\phi_p - \phi_w) = \frac{\Gamma}{\delta x} (2\phi_L - 3\phi_p + \phi_w),$$

$$\frac{\delta x \rho u}{\Gamma} (\phi_p - \phi_w) = (2\phi_L - 3\phi_p + \phi_w),$$

$$\text{Pe} (\phi_p - \phi_w) = (2\phi_L - 3\phi_p + \phi_w) \quad ,$$

$$\text{where: } \text{Pe} = \frac{\delta x \rho u}{\Gamma},$$

$$(1 + \text{Pe})\phi_w + (-3 - \text{Pe})\phi_p = -2\phi_L,$$

apply at point 5:

$$(1 + \text{Pe})\phi_4 + (-3 - \text{Pe})\phi_3 = -2\phi_L,$$

now, we have five equations with five unknowns as follows:

$$(-Pe-3)\phi_1 + \phi_2 = (-Pe-2)\phi_0 \quad \dots (1)$$

$$(1+Pe)\phi_1 + (-2-Pe)\phi_2 + \phi_3 = 0 \quad \dots (2)$$

$$(1+Pe)\phi_2 + (-2-Pe)\phi_3 + \phi_4 = 0 \quad \dots (3)$$

$$(1+Pe)\phi_3 + (-2-Pe)\phi_4 + \phi_5 = 0 \quad \dots (4)$$

$$(1+Pe)\phi_4 + (-3-Pe)\phi_5 = -2\phi_L \quad \dots (5)$$

we can transform these equations to matrix form as follows:

$$\begin{bmatrix} (-Pe-3) & 1 & 0 & 0 & 0 \\ (1+Pe) & (-2-Pe) & 1 & 0 & 0 \\ 0 & (1+Pe) & (-2-Pe) & 1 & 0 \\ 0 & 0 & (1+Pe) & (-2-Pe) & 1 \\ 0 & 0 & 0 & (1+Pe) & (-3-Pe) \end{bmatrix} \begin{bmatrix} \phi_1 \\ \phi_2 \\ \phi_3 \\ \phi_4 \\ \phi_5 \end{bmatrix} = \begin{bmatrix} (-Pe-2)\phi_0 \\ 0 \\ 0 \\ 0 \\ -2\phi_L \end{bmatrix},$$

the coefficient matrix called the tridiagonal matrix that has many features that facilitate access to the solution. This system can be solved in more than one way, like Jacobi, Gauss-Seidel, or the backward direct method. I'm going to solve this system using the Gauss-Seidel method to compare with the previous results of the central-differencing scheme.

MATLAB results: (see Figures E13, E14, E15 and E16 in Appendix E).

3.3 Schemes Comparison

As is the habit when more than one numerical solution method is discussed to solve the same problem or the same equation, to determine which approach is more successful or to identify the benefits and drawbacks of each method independently, it is necessary to compare them using predetermined criteria, and here, since we use numerical methods of solution, which are methods that depend on approximation mainly, stability and accuracy must be discussed for each of the methods to reach the best, and here it is necessary From saying that there may not be a better method than the other in general, but it may be a

better way in terms of stability, but in terms of accuracy, it may not be the best, and vice versa with regard to the other method, it may be better in terms of accuracy, but it is not good in stability.

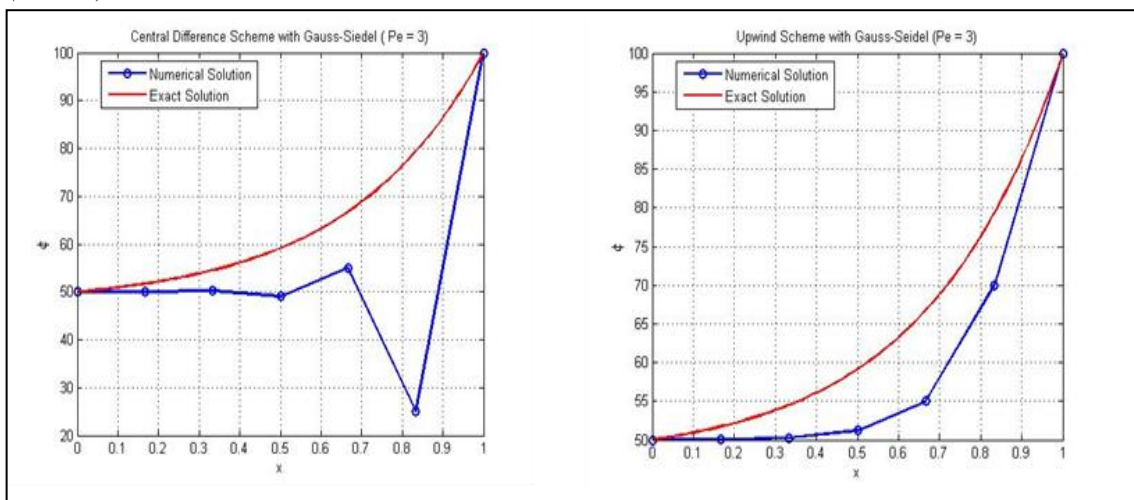
In terms of accuracy, when it comes to numerical diffusion, the central differencing scheme has the upper hand due to its second-order spatial precision for both convection and diffusion terms, whereas the upwind scheme has the upper hand due to its first-order accuracy, especially in diffusion-dominated flows. And since we are talking about accuracy, the central differencing performs better when the diffusion is dominated, because gradients are precisely resolved without the need for numerical dissipation, but the upwind performs better when convection is dominated.

As for stability, the central differencing scheme is stable for $Pe < 2$, but when $Pe > 2$, the scheme can produce oscillations or even instabilities. As for the upwind scheme, it is unconditionally stable for all Peclet numbers; this is what distinguishes this scheme, and one of the advantages of this scheme is that the solution is stabilized for high Peclet numbers ($Pe > 2$) by the numerical dissipation introduced by the upwind scheme.

In the following figure, two graphs generated by the central differencing scheme and the upwind scheme at the same Pe and the same data show the instability for the central differencing scheme and the stability for the upwind scheme at the same Pe .

Figure 3.8

Central Difference Scheme with Gauss-Seidel ($Pe = 3$) and Upwind Scheme with Gauss-Seidel ($Pe = 3$)



So we can say that the central differencing scheme is better when the diffusion is more dominant than the convection ($Pe < 2$) since it has second-order accuracy, but when the convection is more dominant than the diffusion ($Pe > 2$), the central differencing scheme becomes not efficient enough due to the oscillations caused by the instability they produce that leads to using the upwind scheme instead of the central differencing scheme, which is more stable irrespective of Pe .

The weighted upwind scheme is a numerical method used in the finite volume framework to approximate convective fluxes more accurately than the standard upwind scheme. It blends the upwind and central differencing schemes using a weighting factor, allowing better control over numerical diffusion and stability. By adjusting this weight, the scheme can maintain the stability of upwind methods while improving accuracy near smooth solution regions. This makes it particularly useful in solving advection-dominated problems in fluid dynamics, where a balance between accuracy and numerical stability is essential.

Chapter Four

Navier-Stokes Equations By FVM

Here we will discuss the finite volume approach for solving the Navier-Stokes equations, building on our previous work with the diffusion and convection equations. Previous discussion established that they are of greater complexity than the convection and diffusion equations, which are considered a special case of Navier-Stokes equations. The complexity of Navier-Stokes comes from the nonlinearity of the equations, which leads to more complex solutions. The convection and diffusion equations describe the process of transferring a specific property through fluids, but the Navier-Stokes equations are more comprehensive because they include multiple effects such as momentum and pressure, as well as convection and diffusion effects, so we can say they describe the general fluid motion.

4.1 steady-state of Navier-Stokes equation in 1 dimension

As I mentioned earlier at the beginning of my thesis that the equations of Navier-Stokes have several cases, it was necessary to allocate time to talking about a specific case so that things do not diverge and complicate. I will solve the 1D steady-state Navier-Stokes equation for incompressible flow in this portion, much as we solved the convection and diffusion equations.

The governing equation of our case is:

$$\rho u \frac{du}{dx} = -\frac{dp}{dx} + \mu \frac{d^2u}{dx^2}, \dots\dots\dots (34)$$

where: $u(x)$: velocity (the unknown), ρ : Density, μ : Dynamic viscosity, and $\frac{dp}{dx}$:

Pressure gradient.

The goal of our problem here to find velocity distribution $u(x)$ for all nodes including boundaries.

Let's assume that we have a pipe with a fluid with u velocity into the pipe, and we want to mesh for it as follows:

assume $L =$ length of the pipe, $\Delta x = \frac{L}{N}$, N : number of control volumes (assume it 5),

Δx : control volume size, u_0, u_L : boundary conditions (see Figure E17 and Figure E1 in appendix E):

now, we integrate governing equation (34) on the P control volume we get:

$$\int_w^e \rho u \frac{du}{dx} dx = \int_w^e -\frac{dp}{dx} dx + \int_w^e \mu \frac{d^2u}{dx^2} dx,$$

$$\int_{x_{i-1/2}}^{x_{i+1/2}} \rho u \frac{du}{dx} dx = \int_{x_{i-1/2}}^{x_{i+1/2}} -\frac{dp}{dx} dx + \int_{x_{i-1/2}}^{x_{i+1/2}} \mu \frac{d^2u}{dx^2} dx,$$

the convection term ($\rho u \frac{du}{dx}$):

$$\int_{x_{i-1/2}}^{x_{i+1/2}} \rho u \frac{du}{dx} dx = \left[\rho u^2 \right]_{x_{i-1/2}}^{x_{i+1/2}},$$

the diffusion term ($\mu \frac{d^2u}{dx^2}$):

$$\int_{x_{i-1/2}}^{x_{i+1/2}} \mu \frac{d^2u}{dx^2} dx = \mu \left(\frac{\partial u}{\partial x} \Big|_{i+1/2} - \frac{\partial u}{\partial x} \Big|_{i-1/2} \right),$$

the pressure gradient term ($-\frac{dp}{dx}$):

$$\int_{x_{i-1/2}}^{x_{i+1/2}} -\frac{dp}{dx} dx = \left[\frac{\partial p}{\partial x} \right]_{i-1/2}^{i+1/2},$$

then:

$$\left[\rho u^2 \right]_{x_{i-1/2}}^{x_{i+1/2}} = \left[\frac{\partial p}{\partial x} \right]_{i-1/2}^{i+1/2} + \mu \left(\frac{\partial u}{\partial x} \Big|_{i+1/2} - \frac{\partial u}{\partial x} \Big|_{i-1/2} \right), \quad (35)$$

now, we need to approximate these terms, but as we know, there are many schemes for approximation, and each of them has its advantages and disadvantages, suitability for the

applied conditions, and effectiveness and stability. I will take the central differencing scheme as an applied example, but other schemes can be adopted in the solution according to the circumstances. So, the approximations of terms using the central differencing scheme are defined as follows:

at the interior control volumes (2,3,4) (see Figure E3 in Appendix E):

the convection term at the east face is approximated as:

$$\rho u^2 \Big|_e = \rho u^2 \Big|_{i+1/2} \approx \rho \left(\frac{u_i + u_{i+1}}{2} \right)^2,$$

the convection term at the west face is approximated as:

$$\rho u^2 \Big|_w = \rho u^2 \Big|_{i-1/2} \approx \rho \left(\frac{u_{i-1} + u_i}{2} \right)^2,$$

thus, the convection term is:

$$\rho \left(\frac{u_i + u_{i+1}}{2} \right)^2 - \rho \left(\frac{u_{i-1} + u_i}{2} \right)^2,$$

the diffusion term at the east face is approximated as:

$$\frac{\partial u}{\partial x} \Big|_{i+1/2} = \frac{u_{i+1} - u_i}{\Delta x},$$

the diffusion term at the west face is approximated as:

$$\frac{\partial u}{\partial x} \Big|_{i-1/2} = \frac{u_i - u_{i-1}}{\Delta x},$$

thus, the diffusion term is:

$$\frac{\mu}{\Delta x^2} (u_{i+1} - 2u_i - u_{i-1}),$$

the pressure gradient term at the east face is approximated as:

$$-\frac{\partial p}{\partial x} \Big|_{i+1/2} = -\frac{p_{i+1} - p_i}{\Delta x},$$

the pressure gradient term at the west face is approximated as:

$$-\frac{\partial p}{\partial x} \Big|_{i-1/2} = -\frac{p_i - p_{i-1}}{\Delta x},$$

thus, the pressure gradient term is:

$$-\frac{p_{i+1} - p_{i-1}}{2\Delta x},$$

now, if we substitute the diffusive, convective, and pressure gradient terms into the flux balance equation (equation 35), we get the following:

$$\rho \left(\frac{u_i + u_{i+1}}{2} \right)^2 - \rho \left(\frac{u_{i-1} + u_i}{2} \right)^2 = -\frac{p_{i+1} - p_{i-1}}{2\Delta x} + \mu \left(\frac{u_{i+1} - u_i}{\Delta x} - \frac{u_i - u_{i-1}}{\Delta x} \right),$$

$$\frac{\rho}{4} \left((u_i + u_{i+1})^2 - (u_{i-1} + u_i)^2 \right) = -\frac{1}{2\Delta x} (p_{i+1} - p_{i-1}) + \frac{\mu}{\Delta x^2} (u_{i+1} - 2u_i + u_{i-1}),$$

$$\frac{\rho}{4} \left(u_{i+1}^2 + 2u_{i+1}u_i + u_i^2 - \left(u_i^2 + 2u_iu_{i-1} + u_{i-1}^2 \right) \right) = -\frac{1}{2\Delta x} (p_{i+1} - p_{i-1}) + \frac{\mu}{\Delta x^2} (u_{i+1} - 2u_i + u_{i-1}),$$

$$\frac{\rho}{4} \left(u_{i+1}^2 - u_{i-1}^2 \right) = -\frac{1}{2\Delta x} (p_{i+1} - p_{i-1}) + \frac{\mu}{\Delta x^2} (u_{i+1} - 2u_i + u_{i-1}),$$

$$\frac{\rho}{4} \left((u_{i+1} - u_{i-1}) (u_{i+1} + u_{i-1}) \right) = -\frac{1}{2\Delta x} (p_{i+1} - p_{i-1}) + \frac{\mu}{\Delta x^2} (u_{i+1} - 2u_i + u_{i-1}),$$

this is the general form that we can use in the interior points (2, 3, and 4) as follows to get 3 equations:

at point 2:

$$\frac{\rho}{4} \left((u_3 - u_1) (u_3 + u_1) \right) = -\frac{1}{2\Delta x} (p_3 - p_1) + \frac{\mu}{\Delta x^2} (u_3 - 2u_2 + u_1),$$

at point 3:

$$\frac{\rho}{4} \left((u_4 - u_2)(u_4 + u_2) \right) = -\frac{1}{2\Delta x} (p_4 - p_2) + \frac{\mu}{\Delta x^2} (u_4 - 2u_3 + u_2),$$

at point 4:

$$\frac{\rho}{4} \left((u_5 - u_3)(u_5 + u_3) \right) = -\frac{1}{2\Delta x} (p_5 - p_3) + \frac{\mu}{\Delta x^2} (u_5 - 2u_4 + u_3),$$

Now, we will move to apply equation (35) at control volume number 1 called (the west boundary), (see Figure E4 in Appendix E):

$$\left[\rho u^2 \right]_{x_{i-1/2}}^{x_{i+1/2}} = \left[-\frac{\partial p}{\partial x} \right]_{i-1/2}^{i+1/2} + \mu \left(\frac{\partial u}{\partial x} \Big|_{i+1/2} - \frac{\partial u}{\partial x} \Big|_{i-1/2} \right),$$

the value of convection term ρu^2 at the east face is approximated:

$$\rho u^2 \Big|_{i+1/2} \approx \rho \left(\frac{u_1 + u_2}{2} \right)^2,$$

the value of convection term ρu^2 at the west face is approximated:

$$\rho u^2 \Big|_{i-1/2} \approx \rho u_0^2,$$

regarding the diffusion term at the east face is approximated as:

$$\mu \frac{\partial u}{\partial x} \Big|_{i+1/2} \approx \mu \frac{u_2 - u_1}{\Delta x},$$

and the diffusion term at the west face is approximated as:

$$\mu \frac{\partial u}{\partial x} \Big|_{i-1/2} \approx \mu \frac{u_1 - u_0}{\Delta x / 2},$$

regarding the pressure gradient term $\left(-\frac{\partial p}{\partial x} \right)$ at the east face is approximated as:

$$-\frac{\partial p}{\partial x} \Big|_{i+1/2} = -\frac{p_2 - p_1}{\Delta x},$$

regarding the pressure gradient term $(-\frac{\partial p}{\partial x})$ at the west face is approximated as:

$$-\frac{\partial p}{\partial x} \Big|_{i-1/2} = -\frac{p_1 - p_0}{\Delta x / 2} = -\frac{2(p_1 - p_0)}{\Delta x},$$

substitute terms in equation (35) will get:

$$\frac{\rho}{4} \left(\left(\frac{u_1 + u_2}{2} \right)^2 - u_0^2 \right) = -\frac{-2p_0 + 3p_1 - p_2}{\Delta x} + \frac{\mu}{\Delta x} (u_2 - 3u_1 + 2u_0),$$

next, we will move to apply equation (35) at control volume number 5 called (the east boundary), (see Figure E5 in Appendix E):

$$\left[\rho u^2 \right]_{x_{i-1/2}}^{x_{i+1/2}} = \left[-\frac{\partial p}{\partial x} \right]_{i-1/2}^{i+1/2} + \mu \left(\frac{\partial u}{\partial x} \Big|_{i+1/2} - \frac{\partial u}{\partial x} \Big|_{i-1/2} \right),$$

the value of convection term ρu^2 at the east face is approximated:

$$\rho u^2 \Big|_{i+1/2} \approx \rho u_L^2,$$

and the value of convection term ρu^2 at the west face is approximated:

$$\rho u^2 \Big|_{i-1/2} \approx \rho \left(\frac{u_5 + u_4}{2} \right)^2,$$

regarding the diffusion term at the east face is approximated as:

$$\mu \frac{\partial u}{\partial x} \Big|_{i+1/2} \approx \mu \frac{u_L - u_5}{\Delta x / 2},$$

the diffusion term at the west face is approximated as:

$$\mu \frac{\partial u}{\partial x} \Big|_{i-1/2} \approx \mu \frac{u_5 - u_4}{\Delta x},$$

regarding the pressure gradient term $(-\frac{\partial p}{\partial x})$ at the east face is approximated as:

$$-\frac{\partial p}{\partial x} \Big|_{i+1/2} = -\frac{p_L - p_5}{\Delta x / 2} = -\frac{2(p_L - p_5)}{\Delta x},$$

regarding the pressure gradient term $(-\frac{\partial p}{\partial x})$ at the west face is approximated as:

$$-\frac{\partial p}{\partial x} \Big|_{i-1/2} = -\frac{p_5 - p_4}{\Delta x} = -\frac{p_5 - p_4}{\Delta x},$$

substitute terms in equation (35) will get:

$$\frac{\rho}{4} \left(u_L^2 - \left(\frac{u_5 + u_4}{2} \right)^2 \right) = -\frac{p_4 - 3p_5 + 2p_L}{\Delta x} + \frac{\mu}{\Delta x} (2u_L - 3u_5 + u_4),$$

now, we have five equations with five unknowns as follows:

$$\frac{\rho}{4} \left(\left(\frac{u_1 + u_2}{2} \right)^2 - u_0^2 \right) = -\frac{-2p_0 + 3p_1 - p_2}{\Delta x} + \frac{\mu}{\Delta x} (u_2 - 3u_1 + 2u_0) \dots (1)$$

$$\frac{\rho}{4} \left((u_3 - u_1)(u_3 + u_1) \right) = -\frac{1}{2\Delta x} (p_3 - p_1) + \frac{\mu}{\Delta x^2} (u_3 - 2u_2 + u_1) \dots (2)$$

$$\frac{\rho}{4} \left((u_4 - u_2)(u_4 + u_2) \right) = -\frac{1}{2\Delta x} (p_4 - p_2) + \frac{\mu}{\Delta x^2} (u_4 - 2u_3 + u_2) \dots (3),$$

$$\frac{\rho}{4} \left((u_5 - u_3)(u_5 + u_3) \right) = -\frac{1}{2\Delta x} (p_5 - p_3) + \frac{\mu}{\Delta x^2} (u_5 - 2u_4 + u_3) \dots (4)$$

$$\frac{\rho}{4} \left(u_L^2 - \left(\frac{u_5 + u_4}{2} \right)^2 \right) = -\frac{p_4 - 3p_5 + 2p_L}{\Delta x} + \frac{\mu}{\Delta x} (2u_L - 3u_5 + u_4) \dots (5)$$

these equations can be solved using MATLAB programming, where $\mu = 1$,

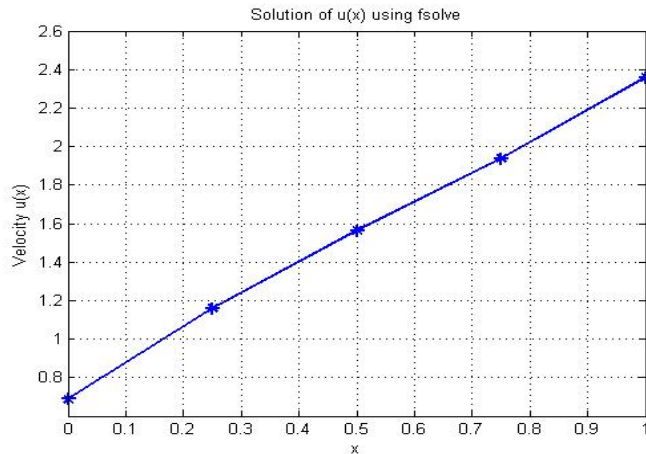
$$\frac{dp}{dx} = 1 - x, \quad \rho = 1, \text{ to get the following result:}$$

$$u(x) = 0.6888 \ 1.1605 \ 1.5621 \ 1.9380 \ 2.3602,$$

(see Figure 4.1):

Figure 4.1

Numerical Solution $u(x)$ using fsolve



4.2 Conclusion

The relevance of fluid dynamics to everyday life and the need to numerically solve certain equations describing fluid motion were discussed in this thesis. This is particularly true given the complexity of these equations and the impossibility of obtaining analytical solutions to them. These numerical solutions were represented by choosing one of the most important numerical methods that are interested in this type of equation, which is the finite volume method. However, it was essential to initially test the effectiveness of this method by examining some cases for which we have analytical solutions, allowing us to compare these with the numerical solutions obtained through its application.

We used the finite volume technique (FVM) to look at how to solve the Navier-Stokes equations numerically, beginning with simple cases by making some assumptions that ignore certain limits in the main equation, and then we gradually made the cases more complex and applied the numerical method. We successfully implemented the discretization and obtained numerical solutions for various boundary conditions. The results were validated against analytical solutions, demonstrating the accuracy and effectiveness of the approach.

Although the numerical approach works, there are some limitations or problems that you may encounter during the solution. In certain circumstances, using this method may lead to instability in the solution; therefore, it is essential to consider selecting the appropriate scheme to prevent these issues. Optimization strategies for adaptive networks or iterative solutions, such as the Gauss-Seidel technique, may also increase computing efficiency.

The situations discussed in this thesis are solved in detail utilizing the approach of restricted volume for the Navier-Stokes equations. Numerical experiments confirm that the method provides reliable approximate estimates and can be expanded to include more complex geometric shapes or practical states that can be described and solved using this method, taking into account and avoiding stability problems.

Through this thesis, future research can focus on addressing some two-dimensional or three-dimensional cases and examining the effectiveness of this numerical approach and applying adaptive network optimization techniques to improve computational efficiency. In addition, the use of high-order schemes to discretize the term convection may enhance the accuracy of the flows of high Peclet numbers, which may open the big door to solving some important problems that were difficult to find analytical solutions to.

List of Abbreviations

Abbreviation	Meaning
FVM	Finite Volume Method
AMR	Adaptive Mesh Refinement
CFD	Computational Fluid Dynamics
R&D	Research and Development
FDM	Finite Difference Method
FEM	Finite Element Method
1D	One-Dimensional
2D	Two-Dimensional
3D	Three-Dimensional
ODEs	Ordinary Differential Equations
PDEs	Partial Differential Equations
LBM	Lattice Boltzmann Method
DNS	Direct Numerical Simulation
LES	Large Eddy Simulation
Pe	Peclet Number

References

- [1]. Versteeg HK. An introduction to computational fluid dynamics the finite volume method, 2/E. Pearson Education India; 2007.
- [2]. Michel Rieutord MR. Fluid Dynamics An Introduction. Springer; 2015.
- [3]. Smolderen JJ. Numerical methods in fluid dynamics. 1978;
- [4]. Niyogi P. Introduction to computational fluid dynamics. Pearson Education India; 2006.
- [5]. Date AW. Introduction to computational fluid dynamics. Cambridge university press; 2005.
- [6]. Hauke G, Moreau R. An introduction to fluid mechanics and transport phenomena. Vol. 86. Springer; 2008.
- [7]. Garvin JW. A student's guide to the Navier-Stokes equations. Cambridge University Press; 2023.
- [8]. Flores J. Applications of the Navier-Stokes equations to wings and complex configurations using a zonal approach. 1988.
- [9]. Jeff Burnham PE. Modeling Dams with Computational Fluid Dynamics: Past Success and New Directions.
- [10]. Ohalete NC, Ayo-Farai O, Onwumere C, Maduka CP, Olorunsogo TO. Navier-stokes equations in biomedical engineering: A critical review of their use in medical device development in the USA and Africa. World Journal of Advanced Research and Reviews. 2024;21(1):1115–31.
- [11]. Li J, Lin X, Chen Z. Finite volume methods for the incompressible Navier-stokes equations. Vol. 2022. Springer; 2022.
- [12]. Bistafa SR. 200 years of the Navier–Stokes equation. Revista Brasileira de Ensino de Física. 2024;46:e20230398.
- [13]. Charnley M. Navier-Stokes Equations: An Introduction. 2014.
- [14]. Axelsson O, He X, Neytcheva M. Numerical solution of the time-dependent Navier–Stokes equation for variable density–variable viscosity. Part I. Mathematical Modelling and Analysis. 2015;20(2):232–60.
- [15]. Mojumder MSH, Haque MN, Alam MJ. Efficient Finite Difference Methods for the Numerical Analysis of One-Dimensional Heat Equation. Journal of Applied Mathematics and Physics. 2023;11(10):3099–123.
- [16]. LeVeque RJ. Finite difference methods for ordinary and partial differential equations: steady-state and time-dependent problems. SIAM; 2007.

- [17]. Jagota V, Sethi APS, Kumar K. Finite element method: an overview. *Walailak Journal of Science and Technology (WJST)*. 2013;10(1):1–8.
- [18]. Cardiff P, Demirdžić I. Thirty years of the finite volume method for solid mechanics. *Archives of Computational Methods in Engineering*. 2021;28(5):3721–80.
- [19]. LeVeque RJ. *Finite volume methods for hyperbolic problems*. Vol. 31. Cambridge university press; 2002.
- [20]. Maliska CR. *Fundamentals of Computational Fluid Dynamics*. Springer; 2023.
- [21]. Yuehgoh F. SECOND ORDER LINEAR ORDINARY DIFFERENTIAL EQUATIONS AND THEIR APPLICATIONS TO THE STUDY OF PROBLEMS IN... 2014;
- [22]. Wang Y, Yu B, Berto F, Cai W, Bao K. Modern numerical methods and their applications in mechanical engineering. *Advances in Mechanical Engineering [Internet]*. 2019 Nov 1;11(11):1687814019887255. Available from: <https://doi.org/10.1177/1687814019887255>
- [23]. Iqbal K, Alam F, Riaz F, Hashmi A, Khalid MN, Gohar A. Application of Numerical Analysis in Real Life. *RN*. 2020;55:7.
- [24]. Burmasheva NV, Prosviryakov EY. Exact solutions to the Navier–Stokes equations describing stratified fluid flows. *Вестник Самарского государственного технического университета Серия «Физико-математические науки»*. 2021;25(3):491–507.
- [25]. Chorin AJ. Numerical solution of the Navier-Stokes equations. *Math Comput*. 1968;22(104):745–62.
- [26]. Sohrabi N, Hammoodi KA, Hammoud A, Jasim DJ, Karouei SHH, Kheyri J, et al. Using different geometries on the amount of heat transfer in a shell and tube heat exchanger using the finite volume method. *Case Studies in Thermal Engineering [Internet]*. 2024 [cited 2025 Feb 13];55:104037. Available from: <https://doi.org/10.1016/j.csite.2024.104037>
- [27]. Anderson D, Tannehill JC, Pletcher RH, Munipalli R, Shankar V. *Computational fluid mechanics and heat transfer*. CRC press; 2020.
- [28]. John D, Anderson JR. *Computational fluid dynamics: the basics with applications*. Mechanical engineering series. 1995;261–2.
- [29]. Blazek J. *Computational fluid dynamics: principles and applications*. Butterworth-Heinemann; 2015.
- [30]. Qin G. *Computational fluid dynamics for mechanical engineering*. CRC Press; 2021.
- [31]. Hauke G, Moreau R. Classification of Fluid Flow. In: Hauke G, editor. *An Introduction to Fluid Mechanics and Transport Phenomena [Internet]*. Dordrecht:

Springer Netherlands; 2008. p. 247–50. Available from:
https://doi.org/10.1007/978-1-4020-8537-6_15

- [32]. Blechta J, Málek J, Rajagopal KR. On the classification of incompressible fluids and a mathematical analysis of the equations that govern their motion. *SIAM Journal on Mathematical Analysis* [Internet]. 2020 [cited 2025 Jan 29];52(2):1232–89. Available from: <https://doi.org/10.1137/19M1244895>
- [33]. Huysmans M, Dassargues A. Review of the use of Péclet numbers to determine the relative importance of advection and diffusion in low permeability environments. *Hydrogeol J* [Internet]. 2005;13(5):895–904. Available from: <https://doi.org/10.1007/s10040-004-0387-4>

Appendices

Appendix A

MATLAB code for ϕ distribution along the rod by the finite volume method example

MATLAB Code:

```
clc; clear; close all;
```

```
%% Problem Definition
```

```
L = 1; % Length of the domain
```

```
N = 40; % Number of control volumes (cells)
```

```
dx = L / (N+1); % Cell size
```

```
x_fvm = linspace(0, L, N+2); % Including boundaries in FVM grid
```

```
phi_0 = 100; % Left boundary condition
```

```
phi_L = 200; % Right boundary condition
```

```
Gamma = 1; % Diffusion coefficient (constant)
```

```
%% Exact Solution (Numerical Calculation)
```

```
x_exact = linspace(0, L, 100); % Fine grid for exact solution
```

```
phi_exact = phi_0 + (phi_L - phi_0) * (x_exact / L); % Direct calculation
```

```
%% Finite Volume Method (FVM) Discretization
```

```
% Define matrix A
```

```
A = diag(2*ones(N,1)) + diag(-1*ones(N-1,1),1) + diag(-1*ones(N-1,1),-1);
```

```
% Modify first and last rows for boundary conditions
```

```
A(1,1) = 1; A(1,2) = 0;
```

```
A(N,N-1) = 0; A(N,N) = 1;
```

```
% Define right-hand side vector b
```

```
b = zeros(N,1);
```

```
b(1) = phi_0;
```

```
b(N) = phi_L;
```

```
% Solve for phi
```

```
phi_internal = A \ b; % MATLAB built-in solver for Ax = b
```

```

% Include boundaries in numerical solution
phi_fvm = [phi_0; phi_internal; phi_L];
%% Plot Results
figure;
plot(x_exact, phi_exact, 'b-', 'LineWidth', 2); hold on;
plot(x_fvm, phi_fvm, 'ro-', 'MarkerSize', 8, 'LineWidth', 2);
xlabel('x');
ylabel('\phi(x)');
title('Exact Solution vs. Finite Volume Method (FVM) with N=40');
legend('Exact Solution', 'FVM Solution', 'Location', 'NorthWest');
grid on;
% Display Numerical Results
disp('FVM Solution including boundaries:');
disp(phi_fvm);

```

Appendix B

MATLAB code for Solving central difference scheme example

```
MATLAB code: central difference scheme
% Parameters
N = 5; % Number of internal nodes
rho = 0.3; % Density (kg/m³)
u = 2.0; % Convection velocity (m/s)
Gamma = 0.1; % Diffusion coefficient (kg/(m·s))
L = 1.0; % Domain length (m)
phi_0 = 50.0; % Boundary condition at left (phi_0)
phi_L = 100.0; % Boundary condition at right (phi_L)
max_iterations = 1000; % Maximum number of Gauss-Seidel iterations
tolerance = 1e-6; % Convergence tolerance

% Grid spacing
dx = L / N; % Grid spacing
Pe = rho * u * dx / Gamma; % Generalized Peclet number

% Initialize coefficient matrix A and RHS vector b
A = zeros(N, N);
b = zeros(N, 1);

% Fill the matrix A and vector b
for i = 1:N
    if i == 1
        A(i, i) = (Pe / 2) + 3;
        A(i, i + 1) = (Pe / 2) - 1;
        b(i) = (2 + Pe) * phi_0;
    elseif i == N
        A(i, i) = -(Pe / 2) + 3;
        A(i, i - 1) = -(Pe / 2) - 1;
        b(i) = (2 - Pe) * phi_L;
    else
        A(i, i - 1) = -(Pe / 2) - 1; % West neighbor
        A(i, i) = 2; % Center coefficient
        A(i, i + 1) = (Pe / 2) - 1; % East neighbor
```

```

end
end
% Initial guess for phi
phi = zeros(N, 1);
% Gauss-Seidel iteration
for iter = 1:max_iterations
    phi_old = phi; % Store old phi values for convergence check

    % Update each phi value using Gauss-Seidel formula
    for i = 1:N
        % Compute the summation for neighbors
        sum_neighbors = 0;
        for j = 1:N
            if j ~= i
                sum_neighbors = sum_neighbors + A(i, j) * phi(j);
            end
        end
        % Update the current value
        phi(i) = (b(i) - sum_neighbors) / A(i, i);
    end

    % Check for convergence
    if norm(phi - phi_old, inf) < tolerance
        disp(['Converged in ', num2str(iter), ' iterations (Gauss-Seidel).']);
        break;
    end
end
% Add boundary conditions to the solution
phi_full = [phi_0; phi; phi_L];
% Compute exact solution
x_exact = linspace(0, L, 100); % Fine grid for exact solution
phi_exact = phi_0 + (phi_L - phi_0) / (exp(Pe) - 1) * (exp(Pe * x_exact) - 1);
% Display results
disp(['Generalized Peclet Number: Pe = ', num2str(Pe)]);
disp('Gauss-Seidel Solution including boundaries (phi_full):');
disp(phi_full);

```

```
% Plot numerical and exact solutions
x = linspace(0, 1, N + 2); % Grid points including boundaries
figure;
plot(x, phi_full, '-o', 'LineWidth', 1.5); hold on;
plot(x_exact, phi_exact, 'r-', 'LineWidth', 1.5);
title(['Central Difference Scheme with Gauss-Siedel (Pe = ' num2str(Pe) ')']);
xlabel('x');
ylabel('\phi');
legend('Numerical Solution', 'Exact Solution', 'Location', 'Best');
grid on;
```

Appendix C

MATLAB code for Solving Upwind scheme example

```
MATLAB code: Upwind scheme
% Parameters
rho = 0.3; % Density (kg/m³)
u = 5; % Convection velocity (m/s)
Gamma = 0.1; % Diffusion coefficient (m²/s)
phi_0 = 50.0; % Boundary condition at x = 0
phi_L = 100.0; % Boundary condition at x = L
N = 5; % Number of internal nodes
L = 1.0; % Domain length (m)
max_iter = 1000; % Maximum number of Gauss-Seidel iterations
tol = 1e-6; % Convergence tolerance

% Compute delta_x and Peclet number (Pe)
dx = L / N; % Spacing between nodes
Pe = rho * u * dx / Gamma; % Using delta_x

% Display local Peclet number
disp(['Local Peclet Number (Pe) = ', num2str(Pe)]);

% Initialize matrix A and right-hand side vector b
A = zeros(N, N);
b = zeros(N, 1);

% Fill the matrix A and vector b based on the given matrix structure
for i = 1:N
    if i == 1
        A(i, i) = -Pe - 3; % First diagonal element
        A(i, i + 1) = 1; % First off-diagonal element to the right
        b(i) = -(Pe + 2) * phi_0; % Right-hand side includes boundary condition phi_0
    elseif i == N
        A(i, i - 1) = 1 + Pe; % Last off-diagonal element to the left
        A(i, i) = -3 - Pe; % Last diagonal element
        b(i) = -2 * phi_L; % Right-hand side includes boundary condition phi_L
    else

```

```

A(i, i - 1) = 1 + Pe; % Off-diagonal element to the left
A(i, i) = -2 - Pe; % Diagonal element
A(i, i + 1) = 1; % Off-diagonal element to the right
end
end

% Gauss-Seidel Method Initialization
phi = zeros(N, 1); % Initial guess for phi

% Gauss-Seidel Iterative Process
for iter = 1:max_iter
    phi_old = phi; % Store old values for comparison
    for i = 1:N
        % Update phi based on Gauss-Seidel formula
        phi(i) = (b(i) - A(i, 1:i-1) * phi(1:i-1) - A(i, i+1:end) * phi_old(i+1:end)) / A(i, i);
    end

    % Check for convergence
    if norm(phi - phi_old, inf) < tol
        fprintf('Converged in %d iterations.\n', iter);
        break;
    end
end

% Include Boundary Conditions
phi_full = [phi_0; phi; phi_L]; % Add boundary values

% Exact Solution Calculation
x_exact = linspace(0, 1, 100); % Fine grid for exact solution
phi_exact = phi_0 + (phi_L - phi_0) / (exp(Pe) - 1) * (exp(Pe * x_exact) - 1);

% Display Results
disp('Solution (phi):');
disp(phi_full);

% Plot Numerical and Exact Solutions
x = linspace(0, 1, N + 2); % Uniform grid including boundaries

```

```
plot(x, phi_full, '-o', 'LineWidth', 1.5); hold on;  
plot(x_exact, phi_exact, 'r-', 'LineWidth', 1.5);  
xlabel('x');  
ylabel('\phi');  
title(['Upwind Scheme with Gauss-Seidel (Pe = ', num2str(Pe), ')']);  
legend('Numerical Solution', 'Exact Solution', 'Location', 'Best');  
grid on;
```

Appendix D

MATLAB code for Solving Navier-Stokes example

solution.m file

```
function FU = solutionU(x)
```

```
L = 1;
```

```
N = 7;
```

```
rho = 1;
```

```
dx = L/5;
```

```
p0 = 1;
```

```
pL = 0.2;
```

```
p = linspace(p0, pL, N);
```

```
p1 = p(2);
```

```
p2 = p(3);
```

```
p3 = p(4);
```

```
p4 = p(5);
```

```
p5 = p(6);
```

```
mu = 0.1;
```

```
uL = 1;
```

```
u0 = 0;
```

```
FU(1) = rho/4*(((x(1)+x(2))/2)^2-u0^2) + (-2*p0+3*p1-p2)/dx - mu/dx*(x(2)-3*x(1)+2*u0);
```

```
FU(2) = rho/4*(x(3)-x(1))*(x(3)+x(1))+1/(2*dx)*(p3-p1)-mu/dx^2*(x(3)-2*x(2)+x(1));
```

```
FU(3) = rho/4*(x(4)-x(2))*(x(4)+x(2))+1/(2*dx)*(p4-p2)-mu/dx^2*(x(4)-2*x(3)+x(2));
```

```
FU(4) = rho/4*(x(5)-x(3))*(x(5)+x(3))+1/(2*dx)*(p5-p3)-mu/dx^2*(x(5)-2*x(4)+x(3));
```

```
FU(5) = rho/4*(uL^2-((x(5)+x(4))/2)^2) + (p4-3*p5+2*pL)/dx - mu/dx*(2*uL-3*x(5)+x(4));
```

solveexactU.m file

```
clear all;
```

```

clc;

% Define initial guess
x0 = zeros(1,5); % Initial guess should match number of equations

% Solve using fsolve
options = optimset('Display', 'iter', 'TolFun', 1e-6, 'TolX', 1e-6);
x = fsolve(@solutionU, x0, options);

% Define x positions for plotting
x_positions = linspace(0, 1, 5);

% Plot the solution
figure;
plot(x_positions, x, '-*', 'LineWidth', 2, 'MarkerSize', 8);
xlabel('x'); ylabel('Velocity u(x)');
title('Solution of u(x) using fsolve');
grid on;

solveUssystem.m file

clear all;
clc;

fun = @solutionU;

x0 = [0,0,0,0,0];

x = fsolve(fun,x0)

%plot(linspace(0, 1, 5),x,'-*')
% Plot the solution
figure;
plot(linspace(0, 1, 5), x, '-*', 'LineWidth', 2, 'MarkerSize', 8);
xlabel('x'); ylabel('Velocity u(x)');
title('Solution of u(x) using fsolve');
grid on;

```

Appendix E

Figures

Figure E.1

Neighbors of P control volume

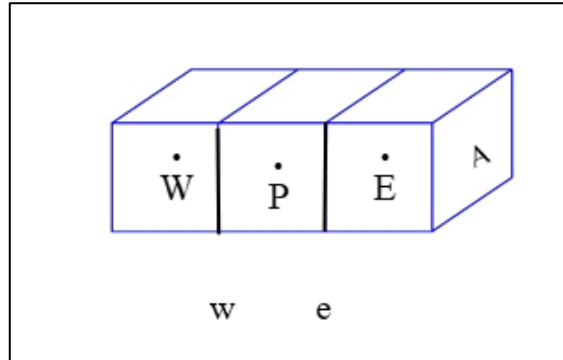


Figure E.2

Division pipe into 5 control Volumes

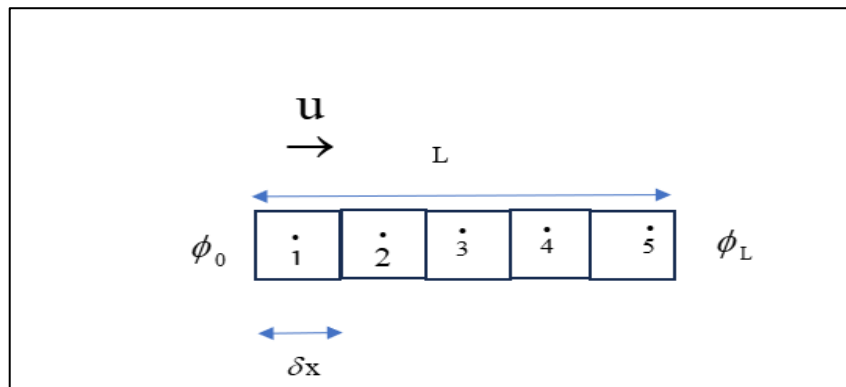


Figure E.3

Interior control volumes

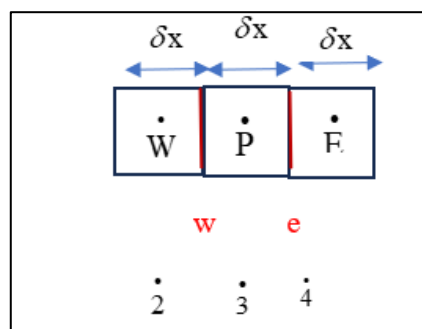


Figure E.4

West Boundary control volume

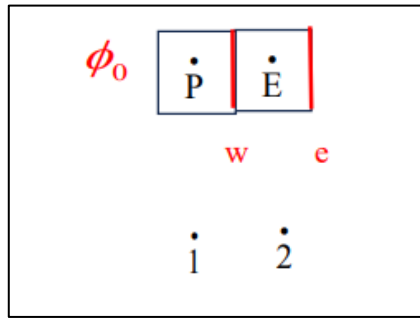


Figure E.5

East Boundary control volume

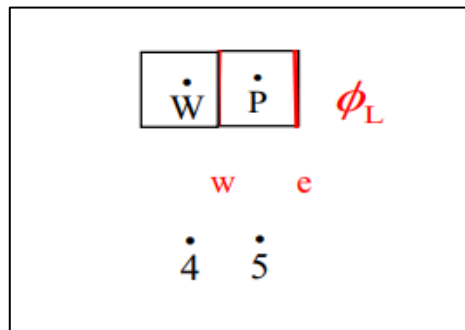


Figure E.6

Central Difference Scheme with Gauss-Siedel ($Pe = 1.2$)

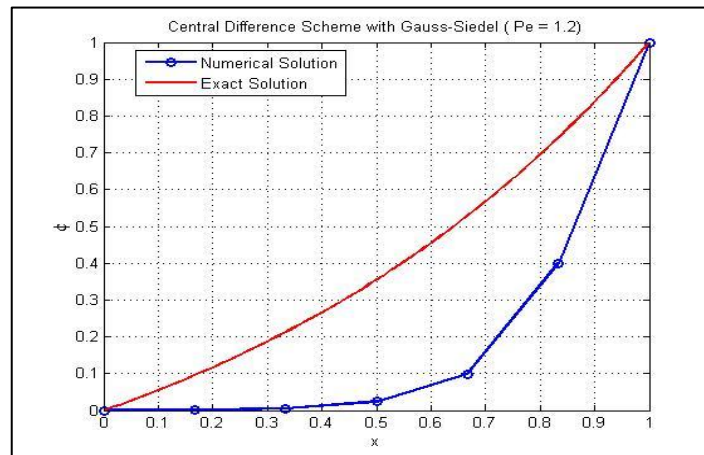


Figure E.7

Central Difference Scheme with Gauss-Siedel ($Pe = 2$)

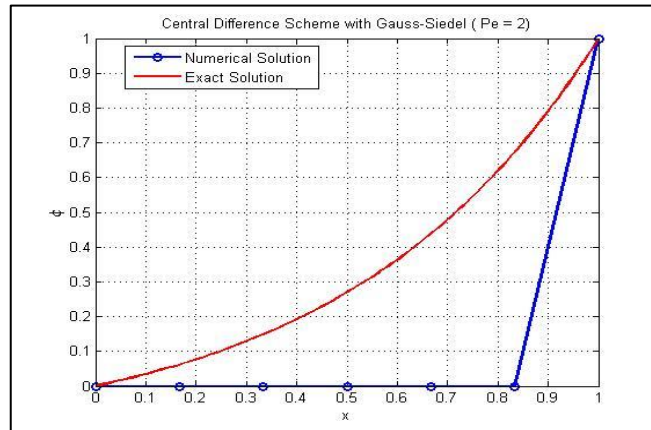


Figure E.8

Central Difference Scheme with Gauss-Siedel ($Pe = 2.4$)

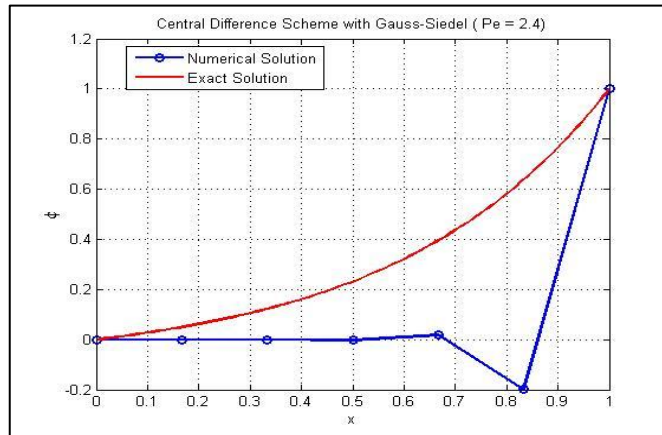


Figure E.9

Central Difference Scheme with Gauss-Siedel ($Pe = 3$)

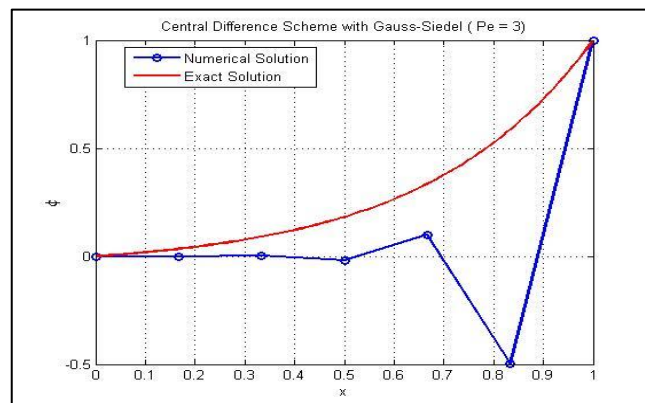


Figure E.10

Interior control volumes

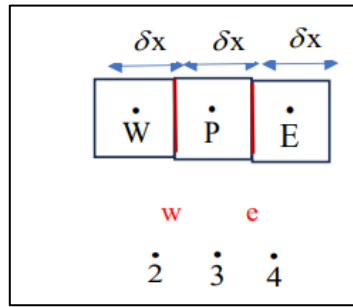


Figure E.11

West Boundary control volume

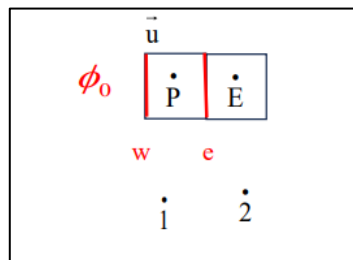


Figure E.12

East Boundary control volume

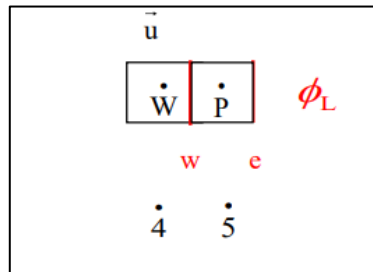


Figure E.13

Upwind Scheme with Gauss-Seidel (Pe = 3)

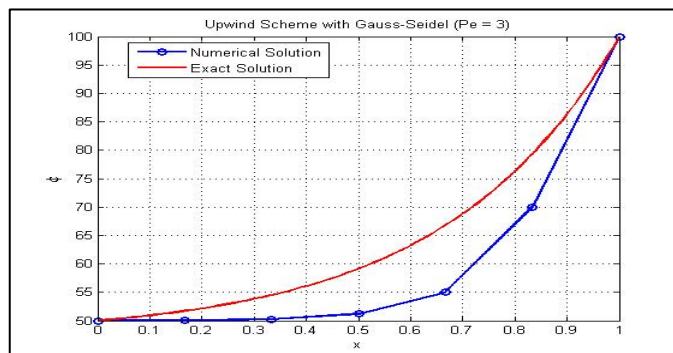


Figure E.14

Upwind Scheme with Gauss-Seidel ($Pe = 2$)

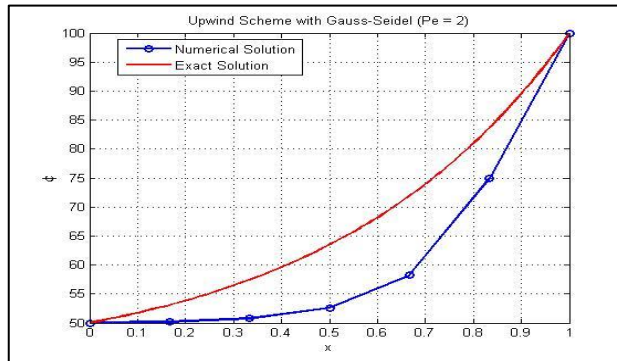


Figure E.15

Upwind Scheme with Gauss-Seidel ($Pe = 5$)

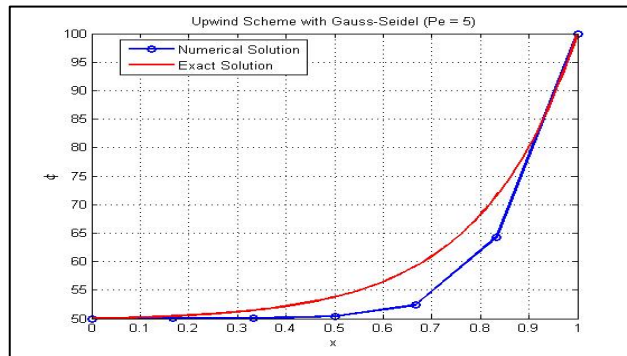


Figure E.16

Upwind Scheme with Gauss-Seidel ($Pe = 1.5$)

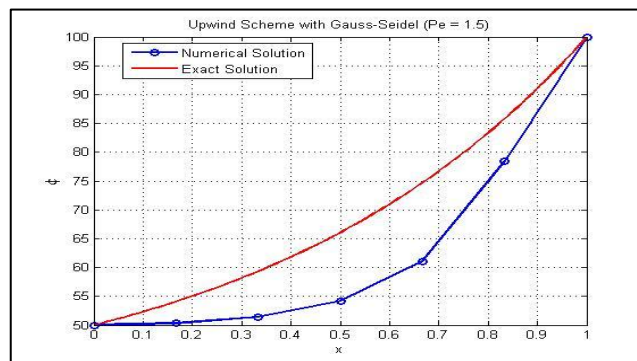
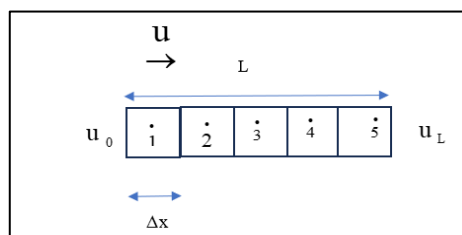


Figure E.17

Division pipe into 5 control Volumes





جامعة النجاح الوطنية
كلية الدراسات العليا

طريقة الحجم المحدود لحل معادلات نافير ستوكس في ديناميكا الموائع

إعداد

عبد الرحيم حسين أبوعرة

إشراف

د. يحيى جعافرة

قدمت هذه الرسالة استكمالاً لمتطلبات الحصول على درجة الماجستير في الرياضيات المحوسبة،
من كلية الدراسات العليا، في جامعة النجاح الوطنية، نابلس - فلسطين.

2025

طريقة الحجم المحدود لحل معادلات نافير-ستوكس في ديناميكا الموائع

إعداد

عبد الرحيم حسين أبوعرة

إشراف

د. يحيى جعافرة

الملخص

تتحكم عدة معادلات، وخاصة معادلات نافير-ستوكس، في ديناميات السوائل. هذه المعادلات ضرورية لوصف حركة السوائل، مما يساعدنا على فهم العديد من الظواهر الطبيعية. تشكل معادلات نافير-ستوكس تحديات كبيرة للباحثين في الرياضيات والهندسة بسبب تعقيدها والصعوبات في الحصول على حلول تحليلية. نتيجة لذلك، أصبح من الضروري استكشاف طرق بديلة لحل هذه المعادلات، لا سيما من خلال الأساليب العددية. نظراً لأن الطرق العددية تنتج حلولاً تقريبية، فمن الضروري تقييم فعالية هذا النهج في معالجة معادلات نافير-ستوكس.

إحدى هذه الطرق العددية هي طريقة الحجم المحدود (FVM)، التي توفر حلولاً تقريبية لمعادلات نافير-ستوكس. في هذه الأطروحة، أجرينا فحصاً شاملاً لطريقة الحجم المحدود باستخدام أمثلة مختلفة من معادلات نافير-ستوكس التي لها حلول تحليلية. بدأنا بحالات أبسط وزدنا التعقيد تدريجياً مع مقارنة نتائجنا العددية بالحلول التحليلية لتقييم مدى توافقها مع الحلول الدقيقة. هذا المقارنة مكنتنا من تقييم فعالية الطريقة.

واجهنا مشاكل تتعلق باستقرار ودقة الحلول العددية بناءً على الظروف المحددة التي فحصناها أثناء استخدام هذه الطريقة. نتيجة لذلك، ناقشنا المخططات العددية المتعلقة بطريقة الحجم المحدود (FVM)

والمعايير لاختيار مخطط معين، خاصة فيما يتعلق برقم بيكلي. ثم قمنا بتقييم فعالية كل مخطط من خلال تطبيقها على نفس الحالة.

النتائج التي تم الحصول عليها من طريقة الحجم المحدود لحل معادلات نافير-ستوكس الثابتة أحادية البعد، مع اختيار مناسب لنظام التمييز، قدمت حلاً دقيقاً مع استقرار ممتاز. ومع ذلك، لاحظنا أنه عند استخدام أرقام بيكلي العالية، ظهرت عدم استقرار في الحل، مما استلزم تنفيذ مخططات تفكيك من الدرجة الأعلى.

يمكن أن يبني البحث المستقبلي على هذه الطريقة من خلال دراسة حالات التدفق في بعدين أو ثلاثة أبعاد وتحسين كفاءة الحوسبة باستخدام تحسين الشبكة التكيفية (AMR) ومخططات التمييز الأفضل.

الكلمات المفتاحية: الحجم المحدود، معادلات نافير-ستوكس، ديناميكا الموائع، مخطط الفرق المركزي، مخطط الاتجاه المواجه، عدد بيكليت، التدفق غير القابل للانضغاط، الحمل الانتشاري، الحل العددي، معادلة الاستمرارية، معادلة الزخم، معادلة الطاقة، المعادلات الحاكمة.